Ann. Inst. H. Poincaré
Anal. Non Linéaire 40 (2023), 1167–1203
DOI 10.4171/AIHPC/63

On hysteresis–reaction–diffusion systems: Singular fast-reaction limit derivation and nonlinear hysteresis feedback

Klemens Fellner and Christian Münch

Abstract. This paper concerns a general class of PDE–ODE reaction–diffusion systems, which exhibits a singular fast-reaction limit towards a reaction–diffusion equation coupled to a scalar hysteresis operator.

As applicational motivation, we present a PDE model for the growth of a population according to a given food supply, coupled to an ODE for the turnover of a food stock. Under realistic conditions the stock turnover is much faster than the population growth, yielding an intrinsic scaling parameter. We present two natural models of consume rate functions such that the dynamics for the food stock converges to a generalised play operator in the associated fast-reaction limit. We emphasise that the structural assumptions on the considered PDE–ODE models are quite general and that analogue systems might describe e.g. cell-biological buffer mechanisms, where proteins are stored and used at the same time.

Finally, we present a new kind of hysteresis–diffusion-driven instability behaviour caused by the nonlinear coupling between a reaction–diffusion equation and a scalar generalised play operator. We discuss in detail how this coupling with a generalised play operator can lead to spatially inhomogeneous large-time behaviour or equilibration to a homogeneous state.

1. Introduction

This paper is concerned with the nonlinear dynamics created by the coupling of a spatially distributed population with a spatially homogeneous stock and the corresponding fast-reaction limit. Let the population be described by a density $v(t,x)$ depending on time $t \geq 0$ and position $x \in \Omega$ within a sufficiently smooth domain $\Omega \subset \mathbb{R}^d$, $d \in \{1,2,3\}$. The total number of individuals is then given by

$$N(t) := \int_\Omega v(t,x)\,dx, \quad t \geq 0.$$

Note the convention that small letters like $v(t,x)$ are used for spatial densities and individual rates, while capital letters like $N(t)$ denote total amounts.

2020 Mathematics Subject Classification. Primary 35K57; Secondary 47J40, 37B55, 35K51.
Keywords. Population dynamics, reaction–diffusion system, fast-reaction limit, hysteresis operator.

The population is assumed to have equal access to an external food supply in terms of a given nonnegative function $F(t) \geq 0$. Alternatively, the population can also resort to food stored in a common stock $S(t) \geq 0$. The time change of the stock is the difference between the food supply F and the total food consumption of the population. The food consumption of each individual is modelled as a nonnegative, locally Lipschitz continuous, food consumption rate $c = c(S, N, F)$ to be detailed later:

$$\varepsilon \dot{S} = F - Nc(S, N, F) = (F - Nc(S, N, F))_+ - (F - Nc(S, N, F))_-, \tag{1}$$

$$S(0) = S_{\text{in}} \geq 0, \tag{2}$$

where $\varepsilon \ll 1$ denotes the timescale of the stock turnover compared to the population dynamics and $(F - Nc)_+$ and $(F - Nc)_-$ denote the usual positive and negative parts.

Equation (1) implies that the population stocks the entire unconsumed food: a somewhat idealistic assumption. The stock loss $(F - Nc)_-$ requires a quasi-positivity condition in order to ensure that stock levels calculated from (1) remain nonnegative, i.e. whenever the stock is empty $S = 0$, then

$$(F - Nc(0, N, F))_- = 0 \quad \text{for all } (N, F) \in (\mathbb{R}^+)^2. \tag{3}$$

Hence, (3) imposes a weak structural constraint on admissible consumption rate functions $c(S, N, F)$.

The growth/decline of the population is described by a growth rate $\lambda(S, N, F)$ of the form

$$\lambda(S, N, F) = \Lambda\Big(\frac{c(S, N, F)}{c_{\min}} - 1\Big), \tag{4}$$

where $\Lambda: \mathbb{R} \mapsto \mathbb{R}$ is a strictly monotone increasing, locally Lipschitz continuous function with $\Lambda(0) = 0$ and $c_{\min}$ denotes the minimal individual consumption required for the population not to decline.

Note that c and λ are assumed spatially homogeneous not only for the sake of the clarity of the presentation but also in view of the hysteresis–diffusion-driven instability, which concerns exactly the destabilisation or stabilisation of a spatially homogeneous large-time dynamics. Note that generalisations to spatially inhomogeneous consumption and growth rates are quite straightforward; see Remark 6 below.

For $T > 0$, the dynamics of the population is modelled by the following (nonlinear) PDE:

$$\partial_t v - D\Delta v = \lambda(S, N, F)v \quad \text{in } [0, T] \times \Omega, \tag{5}$$

$$\partial_\nu v = 0 \quad \text{on } [0, T] \times \partial\Omega, \tag{6}$$

$$v(0) = v_{\text{in}} \geq 0 \quad \text{in } \Omega, \tag{7}$$

where D is a positive diffusion coefficient and ν the outer unit normal. Note that (5)–(7) entail the evolution of the population size $N(t)$:

$$\dot{N}(t) = \lambda(S, N, F)N(t) \ \text{ in } [0, T], \quad N(0) = N_{\text{in}} := \int_\Omega v_{\text{in}}(x)\, dx > 0. \tag{8}$$

Under natural assumptions, yet without requiring any further details on c, the first result of the paper proves existence of strong solutions.

Theorem 1 (Local/global existence and uniqueness of solutions to (1)–(8)). *For $T > 0$, consider a nonnegative food supply $0 \le F(t) \in \mathrm{W}^{1,\infty}(0,T)$. Assume a nonnegative, locally Lipschitz continuous consumption rate $c(S,N,F)\colon (\mathbb{R}^+)^3 \mapsto \mathbb{R}$, which satisfies (3) and extends to a continuous and locally Lipschitz continuous function on $\mathbb{R}^2 \times \mathbb{R}^+$. Assume nonnegative initial data $0 \le S_{\mathrm{in}}$ and $0 \le v_{\mathrm{in}} \in \{v \in \mathrm{H}^2(\Omega) : \partial_\nu v = 0 \text{ on } \partial\Omega\}$ with positive initial population size $0 < N_{\mathrm{in}}$.*

Then, for any $\varepsilon > 0$, the PDE–ODE system (1)–(8) has a unique local solution (v,S) with

$$\begin{aligned} &S \in \mathrm{C}^1([0,T]),\\ &v \in \mathrm{C}\big([0,T];\mathrm{H}^2(\Omega)\big) \cap \mathrm{C}\big((0,T];\mathrm{C}^{2,\beta}(\bar\Omega)\big)\\ &\qquad \cap \mathrm{C}^1\big([0,T];\mathrm{L}^2(\Omega)\big) \cap \mathrm{C}^1\big((0,T];\mathrm{C}^{0,\beta}(\bar\Omega)\big), \end{aligned}$$

which extends globally in time provided that $c(S,N,F)$ (and thus $\lambda(S,N,F)$) is bounded along solutions. Note that any Hölder exponents $0 < \beta < 2 - \frac{d}{2}$ can be chosen by taking s arbitrarily close to 2 in the Sobolev embedding $\mathrm{H}^s(\Omega) \hookrightarrow \mathrm{C}^{0,\beta}(\bar\Omega)$; see proof.

Moreover, solutions to (1)–(8) are nonnegative: $(v(t,x), S(t)) \ge 0$ for all $t \in [0,T]$, $x \in \bar\Omega$.

The main aim of this paper is to rigorously perform the singular fast-reaction limit $\varepsilon \to 0$. Indeed, system (1)–(8) may serve as a simplified model for a human or animal population, which maintains a stock, such as termites, for instance. Populations typically reproduce on a timescale of months/days, yet stock turnover happens on a timescale of hours/minutes, which implies $\varepsilon = O(10^{-3})$. Alternative applications stem from cell biology, where the stock serves as a simple model for a buffer mechanism, which acts to stabilise the concentration of a substance within certain limits; see e.g. [3, 20]. While the separation of timescales in cell biology might be less strong, it is still required for such a buffer mechanism to function.

All other ingredients in system (1)–(8) are set in a very simple way: a spatial homogeneous growth rate; a spatial homogeneous stock and food supply assuming e.g. that the population balances inhomogeneities sufficiently fast to render them negligible; linear diffusion with a spatial homogeneous diffusion constant as the simplest model for the mobility of the population within a fixed domain without influence of the homogeneous food supply. All of these model aspects could certainly be made more realistic when focussing on a particular application and we refer to Remarks 5 and 6 that the results of this paper generalise to many more complicated systems.

Theorem 3 below proves that solutions to system (1)–(8) converge – under natural assumptions on the consumption rate c – in the limit $\varepsilon \to 0$ to solutions (v_0, S_0) to a PDE for v_0 coupled to a hysteresis operator for S_0. The hysteresis operator is a generalised play operator, where admissible states are formed by the graphs of two nondecreasing curves,

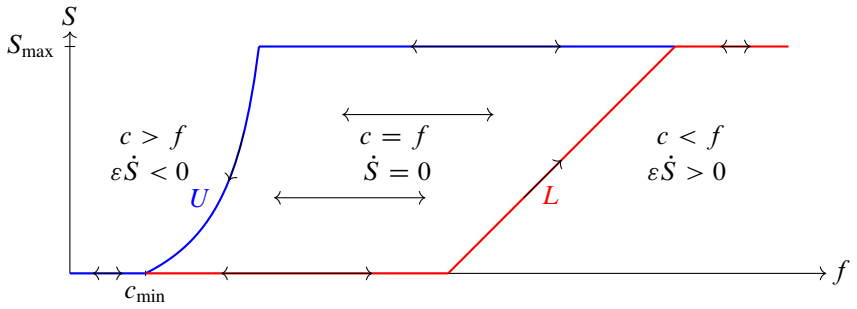

Figure 1. An f–S phase-space diagram of a consumption rate c yielding in the limit $\varepsilon \to 0$ a stock dynamic satisfying a generalised play operator with upper and lower threshold functions U and L.

which may partially overlap; see e.g. [28, Section III.2] or Theorem 3 below for a precise definition as variational inequality. In order to emphasise that Theorem 3 holds for a large class of consumption rates c, we specify here only the structural assumptions which are required to prove Theorem 3 and postpone the details of two examples of consumption rates to Section 2: first we rewrite the stock dynamics (1) in terms of the individual food supply $f = F/N$, i.e.

$$\varepsilon \dot{S} = N(f - c), \quad f(t) := \frac{F(t)}{N(t)},$$

and remark that $f(t)$ is well defined since (8), (4) and the properties of Λ imply $\dot{N} \geq -|\Lambda(-1)|N$ and the ε-independent a priori estimate

$$N(t) \geq N_{in} \exp(-|\Lambda(-1)|t) > 0, \quad t \geq 0. \tag{9}$$

Then Theorem 3 assumes the existence of a connected, closed area of the f–S phase space, where the consumption rate c equals the individual food supply f and the stock remains unchanged $\dot{S} = 0$. In Figure 1 we plot an according, prototypical partition of the f–S phase space in the case that there exists a maximal stock level S_{max}. This area where $c = f$ is given in terms of upper and lower threshold functions $U(f)$ and $L(f)$. Note that the area where $c = f$ may also include one-dimensional lines as shown in Figure 1.

In terms of modelling, the existence of such an area means that the individual food consumption follows – within limits – the individual food supply, by psychological factors and/or by biological factors like metabolic adaptation due to starving/fasting; see e.g. [2, 19, 26].

Furthermore, we consider consumption rates c, which are strictly larger than f to the left of U because individuals supplement the (too) low food supply f by resources of the stock, i.e. $\varepsilon \dot{S} < 0$ until the stock is depleted. On the other side, to the right of L, we suppose $c < f$ and the stock is increased by surplus food, i.e. $\varepsilon \dot{S} > 0$ until S_{max} is reached.

As depicted in Figure 1, we assume that the threshold functions U and L depend on the individual food supply f.

Assumption 2 (Admissible consumption rates c for hysteresis limit). Suppose a nonnegative, locally Lipschitz continuous consumption rate $c(S, N, F)$, which (i) is bounded in N (a natural assumption for an individual rate), (ii) exhibits two locally Lipschitz continuous, monotone increasing threshold functions $U(f)$ and $L(f)$ with a nontrivial area $U(f) > L(f)$ and (iii) takes corresponding values $c > f$, $c = f$ and $c < f$ as sketched in Figure 1. Moreover, assume that there exists an (ε-independent) maximal stock level $S_{\max}$ along solution trajectories.

We emphasise that Assumption 2, in particular the bound $S_{\max}$, together with the assumptions of Theorem 1, in particular $F(t) \in \mathrm{W}^{1,\infty}(0,T)$, and (9), ensures that such a consumption rate $c(S, N, F)$ is bounded independently of ε along the corresponding solutions, which thus extend globally in time.

For the sake of clearly denoting the limit $\varepsilon \to 0$, we use in the following ε-subscripted names for solutions to (1)–(8) with $\varepsilon > 0$, i.e. v_ε, $N_\varepsilon := \int_\Omega v_\varepsilon \, dx$, S_ε and $f_\varepsilon := F/N_\varepsilon$.

Theorem 3 (Singular limit to PDE–hysteresis system). *Suppose the assumptions of Theorem 1 and Assumption 2. The following PDE–hysteresis system admits a unique solution* (v_0, S_0, N_0) *with* $f_0 := F/N_0$*:*

$$\partial_t v_0 - D\Delta v_0 = \lambda(S_0, N_0, F)v_0 \qquad \text{a.e. in } (0,T)\times\Omega, \tag{10}$$

$$\partial_\nu v_0 = 0 \qquad \text{a.e. in } (0,T)\times\partial\Omega, \tag{11}$$

$$v_0(0) = v_{\mathrm{in}} \qquad \text{a.e. in } \Omega, \tag{12}$$

$$S_0(0) = \min\bigl\{\max\{L(f_0(0)), S_{\mathrm{in}}\}, U(f_0(0))\bigr\}, \qquad f_0(0) = F(0)/N_0(0), \tag{13}$$

$$\dot{S}_0(t)(S_0(t) - z) \le 0 \text{ for all } z \in [L(f_0(t)), U(f_0(t))] \qquad \text{a.e. in } [0,T], \tag{14}$$

$$S_0(t) \in [L(f_0(t)), U(f_0(t))] \qquad \text{in } [0,T], \tag{15}$$

$$\dot{N}_0(t) = \lambda(S_0, N_0, F)N_0(t) \qquad \text{in } [0,T],\ N_0(0) = N_{\mathrm{in}}. \tag{16}$$

Here, (13)–(15) *identify* S_0 *as a generalised play operator with input* f_0 *for the curves* U *and* L *and* (16) *follows from integrating* (10)*.*

Then, for all $T > 0$ *and* $2 \le q < \infty$*,* v_0 *has the same regularity as* u_ε *in Theorem 1 and* S_0 *is in* $\mathrm{W}^{1,\infty}(0,T)$*. Finally, in the limit* $\varepsilon \to 0$*,*

$$u_\varepsilon \to v_0 \text{ in } \mathrm{W}^{1,q}(0,T;\mathrm{L}^2(\Omega)) \cap \mathrm{L}^q(0,T;\mathrm{H}^2(\Omega)) \quad \text{and} \quad S_\varepsilon \to S_0 \text{ in } \mathrm{L}^q(0,T)$$

and $S_\varepsilon(t)$ *and* $S_0(t)$ *are uniformly bounded in* t *and* ε *by* $S_\varepsilon(t), S_0(t) \le S_{\max}$ *for all* $t \in [0,T]$*, for all* $\varepsilon > 0$*.*

Remark 4 (Remarks on the existence and uniqueness of the limiting system). The existence and uniqueness of solutions to (10)–(15) is part of Theorem 3. Existence follows by showing that a limit (v_0, S_0, N_0) of $(v_\varepsilon, S_\varepsilon, N_\varepsilon)$ solves (10)–(15). The limit S_0 is a generalised play operator for the Lipschitz continuous curves U and L with input $f_0 = F/N_0$. By

[28, Chapter III.2, Theorem 2.2], this generalised play operator is a Lipschitz continuous hysteresis operator from $C([0,T]) \times \mathbb{R}$ to $C([0,T])$. An alternative existence proof uses a fixed point argument similar to [21, Theorem 3.1]. Crucial for proving uniqueness is the estimate $N_0(t) \geq \delta(T) > 0$ for all $t \in [0,T]$, which follows from (9). Hence, $f_0 = F/N_0$ is Lipschitz continuous and uniqueness of (v_0, S_0, N_0) follows with a Grönwall argument.

Remark 5 (Generalisation to reaction–diffusion-system/ODE–hysteresis models). The semigroup based existence theory of Theorem 1 can be extended to nonlinear reaction–diffusion systems (see e.g. [23, Chapter 6]), where the reaction terms describe nonlinear interactions (like food competition) between different species. For m-species models, the total population size is given by $N(t) = \sum_{i=1}^{m} \int_\Omega v_i(t,x)\,dx$, and we expect that analogous results to Theorem 3 can be proven via similar arguments.

Remark 6 (Generalisation to spatially heterogeneous models). It is also quite straightforward to generalise Theorems 1 and 3 to x-dependent consumption and growth rates. Considering spatially heterogeneous models can be interesting for many applications. Note that models involving x-dependent consumption rates c have to be adapted in the sense that all terms $(f - c)$ have to be replaced by some functional evaluating c, for example by $(f - \int_\Omega vc\,dx/N)$.

Then similar proofs to those stated in this paper also apply to spatially heterogeneous models as long as all functions are sufficiently regular in x and satisfy the correct boundary conditions. For spatially inhomogeneous growth rates λ, we remark that the evolution equation for N also needs changing, for instance,

$$\dot{N}(t) = \int_\Omega \lambda(N(t), F(t), S(t), x) v(x,t)\,dx \geq -\|\lambda(N(t), F(t), S(t), \cdot)\|_{L^\infty(\Omega)} N(t).$$

which generalises the important lower bound (9) for N_ε and N_0 on $[0,T]$ independently of ε.

1.1. Outline and related works

The proof of existence and regularity in Theorem 1 for the consumption and growth rate functions c and λ and for fixed $\varepsilon > 0$ adapts well-known methods of semigroup theory (see e.g. [14, 23]) and is postponed to the final Section 5. Excellent references to the analysis of PDE–hysteresis systems are also the books [5, 28]. More specific references to the well-posedness of reaction–diffusion models with spatially distributed hysteresis are [11, 12], which were used to describe pattern formation of growing colonies of the bacteria *Salmonella typhimurium*; see also [15, 16] for the underlying modelling of the hysteretic interaction of nondiffusive bacteria and diffusive nutrients/proteins.

In Section 2 we present two heuristic consumption rate models and prove that they satisfy the assumptions of Theorems 1 and 3. A first model for c supposes a bounded maximal consumption. As a consequence the stock could build up arbitrarily large, violating the bound $S_{\max}$ in Assumption 2. However, Proposition 7 proves under weak additional

assumptions (on the food supply $F(t)$ and/or the population dynamics in (8)) that the stock remains bounded by a constant $S_{\max}$ along solutions. The second consumption rate model ensures a finite maximal stock level by forcing arbitrarily large consumption (or waste) as stock levels approach $S_{\max}$.

In Section 3 we prove Theorem 3. The proof generalises ideas of a related previous result of ODE–hysteresis system [18]. For further references on multi-scale systems and hysteresis limits we also refer to [27] modelling rate-independent oscillations in molecular dynamical systems and the book [17] and the references therein.

Section 4 studies numerical examples. A first example illustrates Theorem 3 and plots a typical evolution of $S(t)$, $N(t)$ and $F(t)$ of the PDE-hysteresis system (10)–(15) (simulation video as supplementary online material). A second example is constructed in terms of a simple nonlinear PDE–hysteresis model and illustrates that the shape functions U, resp. L of the generalised play operator can decide between spatial homogenisation or unbounded growth of spatially inhomogeneous Fourier modes, a phenomenon which could be called *hysteresis–diffusion-driven instability*. While the presented hysteresis–diffusion-driven instability is – to our knowledge – a newly described phenomenon, there are related references on pattern formation in PDE–hysteresis systems in the context of bacteria colony models [7, 9, 10, 13], describing population dynamics [24] and modelling gravity fingering in porous media [25].

2. Two models of consumption rate functions

In Sections 2.1 and 2.2 we present two prototypical models for consumption rate functions of the form $c = c(S, N, f)$ with $f = F/N$, which each lead to a stock dynamic given by a generalised play operator in the singular limit $\varepsilon \to 0$. In Section 2.3, we prove that both satisfy the assumptions of Theorems 1 and 3. Since both consumption rates $c(S, N, f)$ are autonomous and only depend on time via the arguments $S(t)$, $N(t)$, $f(t)$, we will suppress the time dependency in $c(S, N, f)$.

2.1. A bounded consumption rate function without stock limitation

The function $c_1(S, N, f)$ constitutes a prototypical model for a uniformly bounded consumption rate, i.e. we postulate a maximal possible individual consumption rate $c_{\max} > c_{\min}$ (recall that a minimal consumption $c_{\min} > 0$ is required for the growth rate λ to be nonnegative) such that

$$0 \le c_1(S, N, f) \le c_{\max}.$$

As a consequence, whenever $f(t) > c_{\max}$, not all food can be consumed and the stock level $S(t)$ increases, which is thus potentially unbounded. However, Proposition 7 in Section 2.3 establishes mild suitable assumptions on $F(t)$ and the population dynamics such that $S(t)$ remains bounded by a constant $S_{\max}$ along corresponding solutions and thus satisfies Assumption 2.

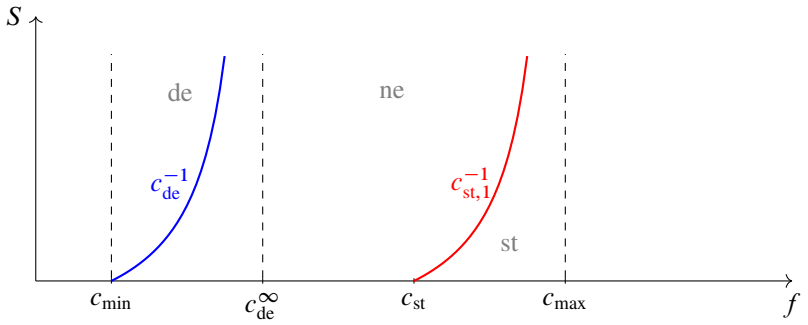

Figure 2. The f–S phase diagram for the consumption rate function c_1 without stock limitation. The lines $S = c_{\mathrm{de}}^{-1}(f)$ and $S = c_{\mathrm{st},1}^{-1}(f)$ separate the depleting, neutral consumption and storing regimes.

We model $c_1(S, N, f)$ as the concatenation of three regions in the f–S phase plane (see Figure 2), which we call the *depleting*, *neutral consumption* and *storing* regimes. Note that while these three regions are characterised by the two variables (f, S), the actual values of c_1 also depend on N.

We state first the regionwise definition of the consumption rate function c_1 before discussing the modelling details:

$$c_1(S,N,f) = \begin{cases} f + \frac{S}{N}\left(1 - e^{-N(1-f/c_{\mathrm{de}}(S))}\right) & \text{if } f < c_{\mathrm{de}}(S), \\ f & \text{if } c_{\mathrm{de}}(S) \le f \le c_{\mathrm{st},1}(S), \\ c_{\mathrm{st},1}(S) & \text{if } f > c_{\mathrm{st},1}(S), \end{cases} \tag{17}$$

where

$$c_{\mathrm{de}}(S) = \frac{c_{\mathrm{de}}^{\infty} S + c_{\min}}{S+1} \quad \text{for some } c_{\mathrm{de}}^{\infty} \in (c_{\min}, c_{\max}) \text{ and } c_{\mathrm{de}}^{-1}(f) = \frac{f - c_{\min}}{c_{\mathrm{de}}^{\infty} - f}, \tag{18}$$

$$c_{\mathrm{st},1}(S) = \frac{c_{\mathrm{st}} + c_{\max} S}{1+S} \quad \text{for some } c_{\mathrm{st}} \in (c_{\mathrm{de}}^{\infty}, c_{\max}) \text{ and } c_{\mathrm{st},1}^{-1}(f) = \frac{f - c_{\mathrm{st}}}{c_{\max} - f}. \tag{19}$$

In the following, we explain the modelling hypothesis leading to the definitions (17), (18) and (19).

Depleting regime. The depleting regime refers to the left-sided area of the f–S phase plane, where the individual food supply f is close to $c_{\min}$ (or below) and the population resorts to supplies from the stock, yet depending on the available stock level S: we fix first an intermediate supply level $c_{\mathrm{de}}^{\infty} \in (c_{\min}, c_{\max})$ and consider situations where the individual food supply f satisfies

$$c_{\min} \le f \le c_{\mathrm{de}}^{\infty} < c_{\max},$$

which means that the total population N is quite large compared to the available food supply F. We then postulate an upper threshold of the depleting regime (i.e. the values of f above which the population stops using the stock) as a monotone increasing function $c_{\mathrm{de}}(S) \in [c_{\min}, c_{\mathrm{de}}^{\infty}]$ as plotted on the left-hand side of Figure 2. If the stock is empty, it is natural to set $c_{\mathrm{de}}(0) = c_{\min}$, which is the critical rate of consumption below which the population declines. A prototypical choice for $c_{\mathrm{de}}(S)$ is the function (18), which saturates at c_{de}^{∞} in the limit $S \to \infty$, yet any strictly monotone C^1 function connecting $(c_{\min}, 0)$ and $(c_{\mathrm{de}}^{\infty}, \infty)$ will yield equivalent results. Note that c_{de}^{∞} is the asymptotically largest consumption rate below which the population enters the depleting regime. It can be interpreted as a model parameter for how carefully the population deals with the stock.

In the depleting regime, the stock consumption for all $S > 0$ yields (recall (1))

$$\varepsilon \dot{S} = -(F - Nc_1)_- = N\big[f - c_1(S, N, f)\big] < 0, \tag{20}$$

since we consider $c_1(S, N, f) > f$ for $S > 0$. In particular, we model c_1 such that $\varepsilon \dot{S} = -l(S, N, f)S$ for some positive, bounded C^1 rate function $l(S, N, f)$. Such a model specifies that the population uses a diminishing stock more carefully in a roughly linear way. We recall that for $S = 0$, we require

$$c_1(0, N, f) = f$$

to satisfy the quasi-positivity condition (3) which means that the population cannot take from an empty stock. This condition entails $c_1(0, N, c_{\min}) = c_{\min} = c_{\mathrm{de}}(0)$. Finally, we wish for $c_1(S, N, f)$ to be continuous in all variables and increasing in S.

All these requirements are satisfied by the following prototypical model for a consumption rate $c_1(S, N, f)$ in the depleting regime, which chooses $l(S, N, f) = 1 - e^{-N(1-f/c_{\mathrm{de}}(S))} \leq 1$, i.e.

$$c_1(S, N, f) = f + \frac{S}{N}(1 - e^{-N(1-f/c_{\mathrm{de}}(S))}) \quad \text{for } f < c_{\mathrm{de}}(S).$$

Storing regime. As second regime, we consider the reverse situation when the food supply F is large compared to the total population N. To define this regime, we introduce an individual consumption level c_{st} such that

$$c_{\mathrm{de}}^{\infty} < c_{\mathrm{st}} < c_{\max}$$

and consider the situation when $f \geq c_{\mathrm{st}}$. Recall that $f \geq c_{\max}$ entails that not all food can be consumed. However, depending on the current stock level S, we postulate that the population decides to store food whenever the individual food supply f surpasses a threshold value $c_{\mathrm{st},1}(S) < c_{\max}$; cf. Figure 2. The storing threshold $c_{\mathrm{st},1}(S)$ is modelled (similarly to $c_{\mathrm{de}}(S)$) as a monotone increasing function of S such that

$$c_{\mathrm{st}} = c_{\mathrm{st},1}(0) \leq c_{\mathrm{st},1}(S) < c_{\max}.$$

One interpretation of c_{st}, which then equals the storing threshold at empty stock, can be as a model parameter of how optimistic the population feels for future food supplies. Moreover, since not all supplied food can be consumed for $f \geq c_{\max}$, it is natural to set $\lim_{S\to\infty} c_{\mathrm{st},1}(S) = c_{\max}$. Hence, a suitable heuristic choice for $c_{\mathrm{st},1}(S)$ is (19), but yet again any such strictly monotone increasing C^1 function will yield equivalent results. Finally, a prototypical (and very simple) model for c_1 in the storing regime is

$$c_1(S, N, f) = c_{\mathrm{st},1}(S) \quad \text{for } f > c_{\mathrm{st},1}(S),$$

which means that the individual consumption c_1 saturates at the maximal level $c_{\mathrm{st},1}(S)$ for all larger food supply rates $f > c_{\mathrm{st},1}(S)$.

Neutral consumption regime. For a medium individual food supply, i.e.

$$c_{\mathrm{de}}(S) \leq f \leq c_{\mathrm{st},1}(S),$$

we assume that the population decides neither to increase nor decrease the stock (although it can be replenished). This is equivalent to saying that the food consumption c_1 adapts to the individual food supply f within those bounds. As mentioned in the introduction, such behaviour might stem from psychological factors and/or biological factors like metabolic adaptation due to starving/fasting; see e.g. [2, 19, 26]. Altogether, we have $\varepsilon \dot{S} = 0 \Leftrightarrow c_1(S, N, f) = f$ in this regime.

2.2. An unbounded consumption rate function ensuring limited stock

As an alternative model to the previous bounded consumption rate, we propose a second consumption rate $c_2(S, N, f)$, which enforces a maximal stock level $S_{\max} > 0$ via potentially unbounded consumption. In this context, unbounded consumption can be interpreted as an unlimited tendency to waste resources in view of a well-filled stock; a behaviour which humans seem to indulge only too easily by forgetting that so many resources are limited. As in the previous subsection, we distinguish three regimes and state the definition of $c_2(S, N, f)$ before discussing the modelling:

$$c_2(S, N, f) = \begin{cases} f + \frac{S}{N}(1 - e^{-N(1-f/c_{\mathrm{de}}(S))}) & \text{if } f < c_{\mathrm{de}}(S), \\ f & \text{if } c_{\mathrm{de}}(S) \leq f \leq c_{\mathrm{st},2}(S), \\ f e^{-(S_{\max}-S)_+} & \\ \quad + c_{\mathrm{st},2}(S)(1 - e^{-(S_{\max}-S)_+}) & \text{if } f > c_{\mathrm{st},2}(S). \end{cases} \tag{21}$$

Depleting regime. We choose the same depleting regime and consumption rate as in Section 2.1: for a $c_{\mathrm{de}}^{\infty} \in (c_{\min}, c_{\max})$, we use $c_{\mathrm{de}}(S)$ as defined in (18) and call the depleting regime all states such that $f < c_{\mathrm{de}}(S)$. In particular, this implies

$$c_2(S, N, f) = f + \frac{S}{N}(1 - e^{-N(1-f/c_{\mathrm{de}}(S))}) \quad \text{for } f < c_{\mathrm{de}}(S).$$

Storing regime. Considering a small population in comparison to the food supply in the sense that $f > c_{\mathrm{st}}$ for a $c_{\mathrm{st}} \in (c_{\mathrm{de}}^{\infty}, c_{\max})$, we postulate (analogously to Section 2.1) a threshold $f = c_{\mathrm{st},2}(S)$, above which the population decides to store food in the stock. Again, it is natural to model $c_{\mathrm{st},2}(S)$ as monotone increasing in S. A simple choice for $c_{\mathrm{st},2}(S)$ which satisfies all our conditions is

$$c_{\mathrm{st},2}(S) = S + c_{\mathrm{st}} \quad \Leftrightarrow \quad c_{\mathrm{st},2}^{-1}(f) = f - c_{\mathrm{st}}. \tag{22}$$

Finally, a maximal stock value $S_{\max}$ is ensured by assuming that the individuals consume/waste the entire individual food supply f once the stock level S has reached $S_{\max}$. A model of a prototypical continuous consumption rate for $f > c_{\mathrm{st},2}(S)$ is given by

$$c_2(S, N, f) = \begin{cases} f e^{S - S_{\max}} + c_{\mathrm{st},2}(S)(1 - e^{S - S_{\max}}) & \text{if } f > c_{\mathrm{st},2}(S) \text{ and } S < S_{\max}, \\ f & \text{if } f > c_{\mathrm{st},2}(S) \text{ and } S \geq S_{\max}. \end{cases}$$

Neutral consumption regime. Identically to Section 2.1, for an individual food supply $c_{\mathrm{de}}(S) \leq f \leq c_{\mathrm{st},2}(S)$, we have $\varepsilon \dot{S} = 0 \Leftrightarrow c_2(S, N, f) = f$.

2.3. Properties of the consumption rate functions c_1 and c_2

The following Proposition 7 and Corollary 9 ensure that both consumption rate models satisfy the requirements of Theorems 1 and 3.

Proposition 7 (A priori bounds on S for consumption rate function c_1). *For fixed $T > 0$ and $F_{\max} := \max_{t \in [0,T]}\{F(t)\}$, $F_{\min} := \min_{t \in [0,T]}\{F(t)\}$, either assume*

$$\|F\|_{C([0,T])} \leq \kappa c_{\max} N_{\mathrm{in}} \exp(-|\Lambda(-1)|T) \quad \text{for some } \kappa \in (0,1) \tag{23}$$

or assume $F_{\max}$, $F_{\min}$, the initial population size N_{in} and Λ in (4) are such that

$$\begin{cases} 0 < F_{\min} \leq F(t) \leq F_{\max} & \text{for all } t \in [0,T], \text{ with } \gamma := \frac{F_{\max}}{F_{\min}} \frac{c_{\min}}{c_{\max}} < 1 \text{ and } N_{\mathrm{in}} \geq \frac{F_{\min}}{c_{\min}}, \\ \Lambda(x) \geq l x & \text{for all } x \geq -1,\ l \geq |\Lambda(-1)|. \end{cases} \tag{24}$$

Then there holds $0 \leq S(t) \leq S_{\max}$ for all $t \in [0,T]$ and $\varepsilon > 0$ with

$$S_{\max} := \max\left\{S_{\mathrm{in}}, \frac{\kappa c_{\max} - c_{\mathrm{st}}}{c_{\max}(1-\kappa)}\right\}, \quad \text{resp. } S_{\max} := \max\left\{S_{\mathrm{in}}, \frac{\gamma - \frac{c_{\mathrm{st}}}{c_{\max}}}{1-\gamma}\right\}.$$

Remark 8. Assumptions (24) allow us to identify an invariant region for (N, S) of the form $N \geq \frac{F_{\min}}{c_{\min}}$ and $S \in [0, \frac{\gamma - c_{\mathrm{st}}/c_{\max}}{1-\gamma}]$. Note that without lower bounds $F_{\min}$ and N_{in}, the population N can become arbitrarily small and that without an upper bound $F_{\max}$ the stock can grow arbitrarily large arbitrarily fast as $\varepsilon \to 0$.

Proof of Proposition 7. Estimate (9) yields, independently of ε,

$$N(t) \geq N_{\mathrm{in}} \exp(-|\Lambda(-1)|T) =: \delta(T) \quad \text{for all } t \in [0,T], \text{ for all } \varepsilon > 0. \tag{25}$$

Thus, by assumption (23), F is uniformly bounded by $\kappa c_{\max}\delta(T)$. Consequently, $f = F/N$ is uniformly bounded by $f \le \kappa c_{\max}$ for all $t \in [0,T]$, for all $\varepsilon > 0$. In the case that $\kappa c_{\max} \le c_{\mathrm{st}}$, it follows that $\dot S \le 0$ in $[0,T]$ since $c_1 \ge f$ holds for $f \le c_{\mathrm{st}}$ in (20). Hence, $S \le S_{\mathrm{in}}$ for all $t \ge 0$ and $\varepsilon > 0$. Otherwise, in the case that $\kappa c_{\max} \in (c_{\mathrm{st}}, c_{\max})$, we have $\dot S \le 0$ if $f \le c_{\mathrm{st},1}(S)$ while $\dot S \ge 0$ provided $f \ge c_{\mathrm{st},1}(S) = \frac{c_{\mathrm{st}}+c_{\max}S}{1+S}$. Only in the second case, we estimate

$$
\begin{aligned}
0 \le \dot S &= \frac{N}{\varepsilon}\Big(f - \frac{c_{\mathrm{st}} + c_{\max}S}{1+S}\Big) \\
&\le \frac{N}{\varepsilon}\Big(\kappa c_{\max} - \frac{c_{\mathrm{st}} + c_{\max}S}{1+S}\Big) = \frac{N(1-\kappa)c_{\max}}{\varepsilon(1+S)}\Big(\frac{\kappa c_{\max} - c_{\mathrm{st}}}{c_{\max}(1-\kappa)} - S\Big),
\end{aligned}
$$

which implies that S is uniformly bounded by $S(t) \le \max\{S_{\mathrm{in}}, \frac{\kappa c_{\max}-c_{\mathrm{st}}}{c_{\max}(1-\kappa)}\}$ for all $t \in [0,T]$, for all $\varepsilon > 0$.

Alternatively, suppose assumption (24). Since N in (8) decays only if $c_1 \le c_{\min}$, which by definition of c_1 only happens if $c_1 \ge f$ also holds, we estimate in such situations that

$$
\dot N = \lambda N \ge \Lambda\Big(\frac{f}{c_{\min}} - 1\Big)N \ge l\Big(\frac{F}{c_{\min}} - N\Big) \ge l\Big(\frac{F_{\min}}{c_{\min}} - N\Big),
$$

where we have used $\Lambda(x) \ge lx$ for some $l \ge |\Lambda(-1)|$. Otherwise N is nondecreasing. Hence, we obtain independently of ε that

$$
N \ge \min\Big\{N_{\mathrm{in}}, \frac{F_{\min}}{c_{\min}}\Big\} = \frac{F_{\min}}{c_{\min}} \quad \text{for all } t \in [0,T], \text{ for all } \varepsilon > 0, \tag{26}
$$

by the assumption on N_{in} in (24). Together with the definition of $\gamma < 1$ in (24), this implies the estimate $f \le F_{\max}/N_{\min} \le \gamma c_{\max}$, which is a sufficient condition to avoid that S grows unboundedly in the limit $\varepsilon \to 0$; see Figure 2. Moreover, we have $\dot S \ge 0$ only if $f \ge c_{\mathrm{st},1}(S) = \frac{c_{\mathrm{st}}+c_{\max}S}{1+S}$. Hence,

$$
\begin{aligned}
\dot S = \frac{N}{\varepsilon}(f - c_{\mathrm{st},1}(S)) &\le \frac{1}{\varepsilon}\Big(F_{\max} - \frac{F_{\min}}{c_{\min}}\frac{c_{\mathrm{st}} + c_{\max}S}{1+S}\Big) \\
&= \frac{F_{\min}c_{\max}}{\varepsilon c_{\min}}\Big(\gamma - \frac{\frac{c_{\mathrm{st}}}{c_{\max}} + S}{1+S}\Big),
\end{aligned}
$$

which implies independently of ε that

$$
S(t) \le \max\Big\{S_{\mathrm{in}}, \frac{\gamma - \frac{c_{\mathrm{st}}}{c_{\max}}}{1-\gamma}\Big\} = \max\Big\{S_{\mathrm{in}}, \frac{\gamma c_{\max} - c_{\mathrm{st}}}{c_{\max}(1-\gamma)}\Big\} \quad \text{for all } t \in [0,T], \text{ for all } \varepsilon > 0.
$$

Note that in the case $c_{\max}\gamma < c_{\mathrm{st}}$, we always have $\dot S \le \varepsilon^{-1}(F_{\max} - \frac{F_{\min}}{c_{\min}}c_{\mathrm{st}}) \le 0$. ∎

Corollary 9 (Admissibility of the consumption rate functions c_1 and c_2). *Consider the consumption rate models $c_1(S,N,f)$ as defined in (17) and with $S_{\max}$ as given by Proposition 7 or $c_2(S,N,f)$ as given in (21) with $S_{\max}$ as in the definition.*

Then c_1 and c_2 satisfy the assumptions of Theorem 1 and Assumption 2. Moreover, with $0 < c_{\min} < c_{\mathrm{de}}^{\infty} < c_{\mathrm{st}} < c_{\max}$, we have as upper and lower threshold functions

$$U(f) = \min\{S_{\max}, u(f)\} \quad \text{with } u(f) := \max\{0, c_{\mathrm{de}}^{-1}(f)\} \text{ and } c_{\mathrm{de}}^{-1}(f) = \tfrac{f - c_{\min}}{c_{\mathrm{de}}^{\infty} - f}$$
$$= \begin{cases} 0, & f \in [0, c_{\min}), \\ \in (0, S_{\max}) \text{ strictly monotone increasing}, & f \in (c_{\min}, \tilde{c}), \\ S_{\max}, & f \geq \tilde{c}, \end{cases} \tag{27}$$

where $\tilde{c} := \frac{S_{\max} c_{\mathrm{de}}^{\infty} + c_{\min}}{S_{\max} + 1}$ is the smallest value where $u(\tilde{c}) = S_{\max}$ holds, and

$$L(f) = \max\{0, l(f)\} \quad \text{with } l(f) := \min\{S_{\max}, c_{\mathrm{st},i}^{-1}(f)\}$$
$$= \begin{cases} 0, & f \in [0, c_{\mathrm{st}}), \\ \in (0, S_{\max}) \text{ strictly monotone increasing}, & f \in (c_{\mathrm{st}}, c_{\mathrm{st},i}(S_{\max})), \\ S_{\max}, & f \geq c_{\mathrm{st},i}(S_{\max}), \end{cases} \tag{28}$$

where $c_{\mathrm{st},i}^{-1}(f)$ is given in (19) or (22) for $i = 1, 2$ and $l(c_{\mathrm{st}}) = 0$.

Proof. In order to verify the assumptions of Theorem 1, we observe first that both consumption rates c_1 and c_2 are piecewise C^1-functions as long as f is well defined, which follows from (9), i.e. $N(t) \geq \delta(T) > 0$ for $t \in [0, T]$ and all $T > 0$ independently of $\varepsilon > 0$. Moreover, c_1 and c_2 are locally Lipschitz continuous in the points where the functions are glued together. Estimate (9) implies furthermore that c_1 and c_2 can be considered as nonnegative, locally Lipschitz continuous in the variable $F \in \mathrm{W}^{1,\infty}(0, T)$ (instead f) independently of ε. Next, both c_1 and c_2 satisfy the quasi-positivity condition (3) by construction and therefore all the assumptions of Theorem 1. Concerning Assumptions 2, c_1 and c_2 are bounded in N by construction. Likewise by construction, they satisfy all the conditions concerning the threshold functions U and L as defined in (27) and (28). Finally, Proposition 7 guarantees the maximal stock level $S_{\max}$. ∎

3. Limit $\varepsilon \to 0$

This section is devoted to the proof of Theorem 3. For the sake of clarity, we will use ε-subscripted names for solutions to (1)–(8) with $\varepsilon > 0$: v_ε, $N_\varepsilon := \int_\Omega v_\varepsilon \, dx$, S_ε and $f_\varepsilon := F/N_\varepsilon$.

A main difficulty in the limit $\varepsilon \to 0$ are bounds lacking on the derivative $\dot{S}_\varepsilon$. One key method of proof is to introduce a projection operator p_ε onto the (ε-independent) area $\dot{S}_\varepsilon = 0$ in the f_ε–S_ε phase-space diagram; cf. [18]. In order to appropriately define this projection p_ε, we require a uniform-in-ε bound on the stock level S_ε.

The main advantage of the projection operator p_ε is to bypass the unbounded derivative of S_ε in the limit $\varepsilon \to 0$. As sketched in Figure 3, the upper and lower threshold

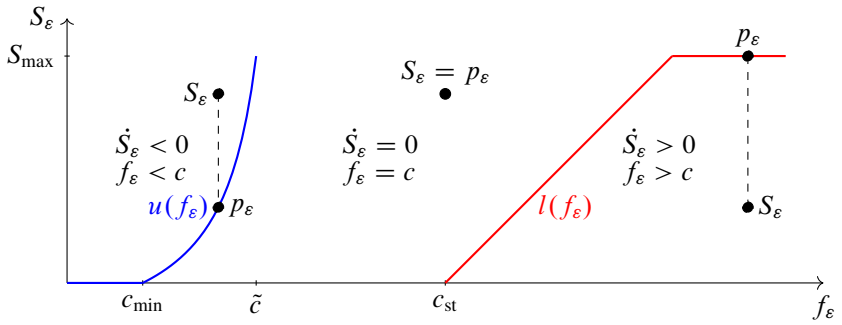

Figure 3. The sign of the derivative of S_ε and projection to p_ε in the f_ε–S_ε phase diagram (for example c_2).

functions $u(f_\varepsilon)$ and $l(f_\varepsilon)$ which envelop the area $\dot{S}_\varepsilon = 0$ have finite slope. Thus, the derivatives of p_ε are bounded in norm independently of ε in terms of the regularity of its driving input variable $f_\varepsilon(t) = F/N_\varepsilon$, i.e. by $F, N_\varepsilon \in \mathrm{W}^{1,\infty}(0,T)$ since N_ε is bounded below independently of $\varepsilon > 0$.

Before we prove Theorem 3, we would like to illustrate in terms of Figure 3 that the limiting stock $S_0(t)$ evolves as a generalised play operator between the curves u and l with input $f_0 = F/N_0$. Note that Figure 3 plots the case of c_2 as defined in Section 2.2; see also (27) and (28) for details.

Let $f_0 = F/N_0$ be a piecewise monotone function on some intervals $[t_1, t_2]$, $[t_2, t_3], \ldots \subset [0, T]$; then S_0 behaves according to the following cases. Consider $f_0(t_1) \in [0, \tilde{c})$ and $S_0(t_1) = u(f_0(t_1))$; then

$$\text{for } t > t_1\text{:} \begin{cases} S_0(t) = u(f_0(t)) & \text{as long as } f_0(t) \text{ decays monotonically in } [0, f_0(t_1)), \\ S_0(t) \equiv S_0(t_1) & \text{as long as } f_0(t) \text{ varies within } (u^{-1}(S_0(t_1)), l^{-1}(S_0(t_1))). \end{cases}$$

If the first case occurs and stops, it starts an instance of the second case. If the second case stops left of the lower threshold l, i.e. $f_0(t_2) < l^{-1}(S_0(t_1))$, it starts a new instance of the second and possibly the first case. We consider rather the new behaviour, which occurs when the second case stops at $S_0(t_1) = l(f_0(t_2))$ for $f_0(t_2) \geq c_{\text{st}}$. Then we have

$$\text{for } t > t_2\text{:} \begin{cases} S_0(t) = l(f_0(t)) \text{ as long as } f_0(t) \text{ increases monotonically in } (f_0(t_2), f_0(t_3)], \\ S_0(t) \equiv S_0(t_2) \quad \text{as long as } f_0(t) \text{ varies within } (u^{-1}(S_0(t_2)), l^{-1}(S_0(t_2))). \end{cases}$$

If the first case occurs and stops, it starts the second case. The stopping of the second case at the upper threshold function u, i.e. $S_0(t_2) = u(f_0(t_3))$, leads back to the first set of two cases with $f_0(t_3) \in [c_{\min}, \tilde{c}]$.

Proof of Theorem 3. We consider a sequence of $\varepsilon > 0$ which tends to zero. We recall that Assumption 2 implies uniform bounds of $S_\varepsilon(t)$ in ε and t, i.e.

$$S_\varepsilon(t) \le S_{\max} > 0 \quad \text{for all } \varepsilon > 0, t \ge 0,$$

and that Proposition 7 proves this for the consumption rate example c_1, while such uniform bounds are true for c_2 by construction. Moreover, by Theorem 1, S_ε is nonnegative independently of ε.

Let $p_\varepsilon(S_\varepsilon, N_\varepsilon, F)$ be the following projection operator in the f_ε–S_ε phase space, cf. Figure 3:

$$p_\varepsilon(S_\varepsilon, f_\varepsilon) := \begin{cases} l(f_\varepsilon) & \text{if } S_\varepsilon \le l(f_\varepsilon), \\ u(f_\varepsilon) & \text{if } S_\varepsilon \ge u(f_\varepsilon) \text{ and } f_\varepsilon \le \tilde{c}, \text{ where } u(\tilde{c}) = S_{\max}, \\ S_\varepsilon & \text{otherwise.} \end{cases} \tag{29}$$

Note that $0 \le S_\varepsilon \le S_{\max}$ implies $0 \le p_\varepsilon \le S_{\max}$. In particular, $p_\varepsilon(S_\varepsilon, f_\varepsilon) = 0 < S_\varepsilon$ follows from downwards projections, whereas $p_\varepsilon(S_\varepsilon, f_\varepsilon) = S_{\max} > S_\varepsilon$ follows from upwards projections.

We divide the proof of the theorem into six steps.

Step 1: Boundedness of N_ε and p_ε in $W^{1,\infty}(0,T)$ independently of $\varepsilon > 0$. As remarked in the introduction, Assumption 2 ensures that $c(S, N, F)$ is bounded along solutions independently of ε. Hence, since Λ in (4) is locally Lipschitz, we see that $\lambda = \Lambda(c(S, N, F)/c_{\min} - 1)$ is also bounded independently of ε. Next, a Grönwall argument applied to (8), i.e. $\dot{N} = \lambda N$, yields boundedness of $N_\varepsilon \in C([0,T]) \cap C^1(0,T)$ independently of ε. Moreover, estimate (9) implies that $f_\varepsilon = F/N_\varepsilon$ is Lipschitz continuous on $[0,T]$ with a modulus L independent of ε. Since u and l are Lipschitz continuous on $[0,\tilde{c}]$ and $[c_{\mathrm{st}}, \infty)$ respectively, we conclude that $u(f_\varepsilon)$ is Lipschitz continuous for $f_\varepsilon \in [0,\tilde{c}]$ and $l(f_\varepsilon)$ is Lipschitz continuous for $f_\varepsilon \in [c_{\mathrm{st}}, \infty)$.

Next we choose $\delta > 0$ sufficiently small such that for all $t_1, t_2 \in [0,T]$ with $|t_1 - t_2| < \delta$ there holds

$$|f_\varepsilon(t_1) - f_\varepsilon(t_2)| \le L|t_1 - t_2| < \frac{c_{\mathrm{st}} - \tilde{c}}{2}. \tag{30}$$

Let $t_0 \in [0,T]$ be given. The definition of p_ε implies that $p_\varepsilon(t_0) = S_\varepsilon(t_0)$ and $\dot{p}_\varepsilon(t_0) = \dot{S}_\varepsilon(t_0) = 0$ almost surely whenever $f_\varepsilon \in [0,\tilde{c}]$ and $S_\varepsilon(t_0) < u(f_\varepsilon(t_0))$ or $\tilde{c} \le f_\varepsilon(t_0) \le c_{\mathrm{st}}$ or $f_\varepsilon > c_{\mathrm{st}}$ and $S_\varepsilon(t_0) > l(f_\varepsilon(t_0))$; see also Figure 3.

Moreover, if $f_\varepsilon(t_0) < \tilde{c}$, then (30) yields $f_\varepsilon(t) < c_{\mathrm{st}}$ on $[t_0, t_0 + \delta]$. Hence, since $S_\varepsilon \ge 0$, in this case $p_\varepsilon(t) = \min\{u(f_\varepsilon(t)), S_\varepsilon(t)\}$ in $[t_0, t_0 + \delta]$, and for a.e. $t \in [t_0, t_0 + \delta]$ there holds

$$f_\varepsilon(t_0) < \tilde{c} \;\Rightarrow\; \dot{p}_\varepsilon(t) = \begin{cases} \dfrac{d}{dt} u(f_\varepsilon)(t) & \text{if } u(f_\varepsilon(t)) \le S_\varepsilon(t), \\ 0 & \text{if } u(f_\varepsilon(t)) > S_\varepsilon(t), \end{cases} \quad \text{on } [t_0, t_0 + \delta].$$

As a consequence, $\dot{p}_\varepsilon$ is bounded a.e. on $[t_0, t_0 + \delta]$ independently of ε.

Finally, the case when $f_\varepsilon(t_0) > c_{\mathrm{st}}$ is treated analogously. Consequently, p_ε is bounded in $\mathrm{W}^{1,\infty}(0,T)$ independently of $\varepsilon > 0$.

Step 2: Convergence of $S_\varepsilon - p_\varepsilon$ to zero in $\mathrm{L}^q(0,T)$ for arbitrary $q \in (1,\infty)$. For arbitrary $\varepsilon > 0$ and $t \in [0,T]$ we have

$$\begin{aligned}
&|S_\varepsilon(t) - p_\varepsilon(t)| \\
&\quad = |S_\varepsilon(0) - p_\varepsilon(0)| + \int_0^t (\dot S_\varepsilon(\tau) - \dot p_\varepsilon(\tau)) \frac{S_\varepsilon(\tau) - p_\varepsilon(\tau)}{|S_\varepsilon(\tau) - p_\varepsilon(\tau)|}\, d\tau \\
&\quad = |S_\varepsilon(0) - p_\varepsilon(0)| + \int_0^t \underbrace{\dot S_\varepsilon(\tau) \frac{S_\varepsilon(\tau) - p_\varepsilon(\tau)}{|S_\varepsilon(\tau) - p_\varepsilon(\tau)|}}_{\le 0}\, d\tau - \int_0^t \dot p_\varepsilon(\tau) \frac{S_\varepsilon(\tau) - p_\varepsilon(\tau)}{|S_\varepsilon(\tau) - p_\varepsilon(\tau)|}\, d\tau,
\end{aligned}$$

where the above inequality follows from the definition of p_ε for all τ; see Figure 3. Hence,

$$\begin{aligned}
&|S_\varepsilon(t) - p_\varepsilon(t)| + \int_0^t \left| \dot S_\varepsilon(\tau) \frac{S_\varepsilon(\tau) - p_\varepsilon(\tau)}{|S_\varepsilon(\tau) - p_\varepsilon(\tau)|} \right| d\tau \\
&\qquad \le |S_\varepsilon(0) - p_\varepsilon(0)| + \int_0^t |\dot p_\varepsilon(\tau)|\, d\tau, \qquad (31)
\end{aligned}$$

and the bounds of Step 1 imply that the right-hand side of (31) and thus $|S_\varepsilon(t) - p_\varepsilon(t)|$ is bounded independently of ε. Similarly, we calculate

$$\begin{aligned}
&(S_\varepsilon(t) - p_\varepsilon(t))^2 - 2\int_0^t \dot S_\varepsilon(\tau)(S_\varepsilon(\tau) - p_\varepsilon(\tau))\, d\tau \\
&\qquad = (S_\varepsilon(0) - p_\varepsilon(0))^2 - 2\int_0^t \dot p_\varepsilon(\tau)(S_\varepsilon(\tau) - p_\varepsilon(\tau))\, d\tau.
\end{aligned}$$

For $t = T$, the above boundedness of $|S_\varepsilon - p_\varepsilon|$ and $\dot p_\varepsilon$ (see Step 1) together with $\dot S_\varepsilon(\tau)(S_\varepsilon(\tau) - p_\varepsilon(\tau)) \le 0$ yields that $\dot S_\varepsilon(S_\varepsilon - p_\varepsilon)$ is bounded in $L^1(0,T)$ independently of ε. Hence,

$$\varepsilon \|\dot S_\varepsilon(S_\varepsilon - p_\varepsilon)\|_{L^1(0,T)} \xrightarrow{\varepsilon\to 0} 0 \quad \Rightarrow \quad \varepsilon \dot S_\varepsilon(\tau)(S_\varepsilon(\tau) - p_\varepsilon(\tau)) \xrightarrow{\varepsilon\to 0} 0 \ \text{ for a.e. } \tau \in (0,T).$$

By inserting $\varepsilon \dot S_\varepsilon = F - c N_\varepsilon$, it follows that

$$\big[F(\tau) - c(S_\varepsilon(\tau), N_\varepsilon(\tau), F(\tau))N_\varepsilon(\tau)\big](S_\varepsilon(\tau) - p_\varepsilon(\tau)) \xrightarrow{\varepsilon\to 0} 0 \quad \text{a.e. } \tau \in (0,T),$$

which implies $S_\varepsilon(\tau) - p_\varepsilon(\tau) \xrightarrow{\varepsilon\to 0} 0$ whenever the term

$$\big[F(\tau) - c(S_\varepsilon(\tau), N_\varepsilon(\tau), F(\tau))N_\varepsilon(\tau)\big]$$

is bounded away from zero. However, when supposing

$$\big[F(\tau) - c(S_\varepsilon(\tau), N_\varepsilon(\tau), F(\tau))N_\varepsilon(\tau)\big] = \big[f_\varepsilon(\tau) - c(S_\varepsilon(\tau), N_\varepsilon(\tau), F(\tau))\big]N_\varepsilon(\tau) \xrightarrow{\varepsilon\to 0} 0,$$

it follows from $N_\varepsilon(\tau) > \delta(T) > 0$ and the definition of p_ε, i.e. $p_\varepsilon = S_\varepsilon \Leftrightarrow f_\varepsilon = c$, that again $S_\varepsilon(\tau) - p_\varepsilon(\tau) \to 0$ as $\varepsilon \to 0$. Finally, since $|S_\varepsilon(\tau) - p_\varepsilon(\tau)| \le 2S_{\max}$, Lebesgue's dominated convergence theorem yields that $S_\varepsilon - p_\varepsilon$ converges to zero in $\mathrm{L}^q(0,T)$ for arbitrary $q \in (1,\infty)$.

Step 3: Weak convergence of a subsequence $\varepsilon \to 0$ and compact embeddings. We recall from Step 1 that since $0 \le S_\varepsilon \le S_{\max}$, $F \in \mathrm{W}^{1,\infty}(0,T)$ and $N_\varepsilon > \delta(T)$ hold independently of ε, the growth rate function $\lambda(S_\varepsilon, N_\varepsilon, F) = \Lambda(c/c_{\min} - 1)$ is bounded independently of ε, which implies that N_ε is bounded in $C([0,T])$ independently of ε. Moreover, the norms of $f_\varepsilon \in \mathrm{W}^{1,\infty}(0,T)$ are bounded independently of ε. Also, $0 \le S_\varepsilon \le S_{\max}$ implies that S_ε is bounded with respect to the sup norm in $C([0,T])$, independently of ε. Moreover, with λ bounded independently of ε, the proof of Theorem 1 in Section 5 (see e.g. (45) and (46)) yields that the norm of v_ε is bounded independently of ε in the following solution space:

$$\mathrm{C}\big([0,T];\mathrm{H}^2(\Omega)\big) \cap \mathrm{C}\big((0,T];\mathrm{C}^{2,\beta}(\bar\Omega)\big) \cap \mathrm{C}^1\big([0,T];\mathrm{L}^2(\Omega)\big) \cap \mathrm{C}^1\big((0,T];\mathrm{C}^{0,\beta}(\bar\Omega)\big),$$

which embeds continuously into $\mathrm{W}^{1,\infty}(0,T;\mathrm{L}^2(\Omega)) \cap \mathrm{L}^\infty(0,T;\mathrm{H}^2(\Omega))$. Also, by Step 1, p_ε is bounded in $\mathrm{W}^{1,\infty}(0,T)$ independently of ε.

Consequently, we can extract a subsequence $\{\varepsilon_k\}_k$ and find some

$$S_0 \in \mathrm{L}^q(0,T) \quad \text{and} \quad v_0 \in \mathrm{W}^{1,q}(0,T;\mathrm{L}^2(\Omega)) \cap \mathrm{L}^q(0,T;\mathrm{H}^2(\Omega))$$

such that $(p_{\varepsilon_k}, v_{\varepsilon_k})$ converges to (S_0, v_0) weakly in those spaces.

Next we use the following embeddings, where $(\cdot,\cdot)_{\eta,1}$ denotes real interpolation:

$$\begin{aligned}
\mathrm{W}^{1,q}((0,T);\mathrm{L}^2(\Omega)) \cap \mathrm{L}^q((0,T);\mathrm{H}^2(\Omega)) &\hookrightarrow\!\!\!\!\!\!\to \mathrm{C}^\beta((0,T);(\mathrm{L}^2(\Omega),\mathrm{H}^2(\Omega))_{\eta,1}) \\
&\hookrightarrow \mathrm{C}^\beta([0,T];\mathrm{L}^2(\Omega)), \\
\mathrm{W}^{1,q}((0,T);\mathrm{L}^2(\Omega)) \cap \mathrm{L}^q((0,T);\mathrm{H}^2(\Omega)) &\hookrightarrow\!\!\!\!\!\!\to \mathrm{C}([0,T];(\mathrm{L}^2(\Omega),\mathrm{H}^2(\Omega))_{\eta,q}) \\
&\hookrightarrow \mathrm{C}([0,T];\mathrm{L}^2(\Omega)),
\end{aligned}$$

for every $0 < \eta < 1 - 1/q$ and $0 \le \beta < 1/q' - \eta$; see e.g. [1, Theorem 3]. Moreover, $\mathrm{W}^{1,q}(0,T)$ is compactly embedded into $\mathrm{C}([0,T])$.

Hence, v_{ε_k} converges strongly to v_0 in $\mathrm{C}([0,T];\mathrm{L}^2(\Omega))$ and thus N_{ε_k} converges strongly to $N_0 = N(v_0)$ in $\mathrm{C}([0,T])$ while p_ε converges strongly to S_0 in $\mathrm{C}([0,T])$. Since by Step 2, $S_\varepsilon - p_\varepsilon$ converges to zero in $\mathrm{L}^q(0,T)$ as $\varepsilon \to 0$, we obtain

$$S_{\varepsilon_k} \xrightarrow{k\to\infty} S_0 \quad \text{in } \mathrm{L}^q(0,T).$$

Step 4: (S_0, v_0) solves the limiting system (10)–(15) and strong convergence. Recall the growth rate (4), i.e. $\lambda(S,N,F) = \Lambda(c(S,N,F)/c_{\min} - 1)$ for a locally Lipschitz continuous function Λ. We will first show by Step 3 and dominated convergence that

$$\Lambda\Big(\frac{c(S_{\varepsilon_k}, N_{\varepsilon_k}, F)}{c_{\min}} - 1\Big) v_{\varepsilon_k} \xrightarrow{\varepsilon_k \to 0} \Lambda\Big(\frac{c(S_0, N_0, F)}{c_{\min}} - 1\Big) v_0 \quad \text{in } \mathrm{L}^q((0,T);\mathrm{L}^2(\Omega)). \tag{32}$$

Indeed, by Step 3 the subsequence v_{ε_k} converges to v_0 in $\mathrm{C}([0,T];\mathrm{L}^2(\Omega))$. Moreover, for a further subsequence ε_k (again denoted by ε_k), it follows from $S_{\varepsilon_k} \to S_0$ in $\mathrm{L}^q(0,T)$ that

$$\Lambda\Big(\frac{c(S_{\varepsilon_k}(t),N_{\varepsilon_k}(t),F(t))}{c_{\min}}-1\Big) \xrightarrow{\varepsilon_k\to 0} \Lambda\Big(\frac{c(S_0(t),N_0(t),F(t))}{c_{\min}}-1\Big) \quad \text{a.e. in } [0,T],$$

where we have used that c is locally Lipschitz continuous due to $N_\varepsilon(t), N_0(t) > \delta(T) > 0$ and $F(t) \geq 0$ and also that Λ is locally Lipschitz continuous. Together with $v_{\varepsilon_k}(x,t) \to v_0(x,t)$ for all $t \in [0,T]$ and a.e. $x \in \Omega$ (w.l.o.g. for the same subsequence ε_k), we obtain

$$\Lambda\Big(\frac{c(S_{\varepsilon_k}(t),N_{\varepsilon_k}(t),F(t))}{c_{\min}}-1\Big)v_{\varepsilon_k}(x,t) \xrightarrow{\varepsilon_k\to 0} \Lambda\Big(\frac{c(S_0(t),N_0(t),F(t))}{c_{\min}}-1\Big)v_0(x,t)$$

for a.e. $t \in [0,T]$ and a.e. $x \in \Omega$. Moreover, by Assumption 2, $c(S_{\varepsilon_k}, N_{\varepsilon_k}, F)$ is uniformly bounded in $[0,T]$ and this estimate also holds when S_{ε_k} is replaced by any S with $0 \leq S \leq S_{\max}$. Hence, $c(S_0,N_0,F)$ also is uniformly bounded in $[0,T]$. Since Λ is locally Lipschitz continuous, it follows that $|\Lambda(c(S_{\varepsilon_k},N_{\varepsilon_k},F)/c_{\min}-1)| \leq C$ and $|\Lambda(c(S_0,N_0,F)/c_{\min}-1)| \leq C$ uniformly in $[0,T]$ for some $C > 0$ independent of ε. Therefore, since $v_{\varepsilon_k}(.,t)$ and $v_0(.,t)$ have a common upper bound in $\mathrm{L}^2(\Omega)$ by Step 3, Lebesgue's dominated convergence theorem yields for a.e. $t \in [0,T]$,

$$\Big\|\Lambda\Big(\frac{c(S_{\varepsilon_k}(t),N_{\varepsilon_k}(t),F(t))}{c_{\min}}-1\Big)v_{\varepsilon_k}(\cdot,t) - \Lambda\Big(\frac{c(S_0(t),N_0(t),F(t))}{c_{\min}}-1\Big)v_0(\cdot,t)\Big\|_{\mathrm{L}^2(\Omega)} \to 0$$

as $\varepsilon_k \to 0$. Finally, since this sequence is also bounded uniformly in $t \in [0,T]$, using Lebesgue's dominated convergence theorem again implies convergence in $\mathrm{L}^q(0,T)$ and thus (32).

Next we observe that the Neumann realisation of $-D\Delta$ satisfies maximal parabolic Sobolev regularity on $\mathrm{L}^2(\Omega)$; see e.g. [8, Theorem 2.9] as a recent state-of-the-art reference. As a consequence,

$$v_{\varepsilon_k} = (\partial_t - D\Delta)^{-1}\Lambda\Big(\frac{c(S_{\varepsilon_k},N_{\varepsilon_k},F)}{c_{\min}}-1\Big)v_{\varepsilon_k} \xrightarrow{\varepsilon_k\to 0} (\partial_t - D\Delta)^{-1}\Lambda\Big(\frac{c(S_0,N_0,F)}{c_{\min}}-1\Big)v_0$$

in $\mathrm{W}^{1,q}((0,T);\mathrm{L}^2(\Omega)) \cap \mathrm{L}^q((0,T);\mathrm{H}^2(\Omega))$. Indeed, since v_{ε_k} converges to v_0 in $\mathrm{L}^q((0,T);\mathrm{L}^2(\Omega))$, this shows

$$v_0 = (\partial_t - D\Delta)^{-1}\Lambda\Big(\frac{c(S_0,N_0,F)}{c_{\min}}-1\Big)v_0$$

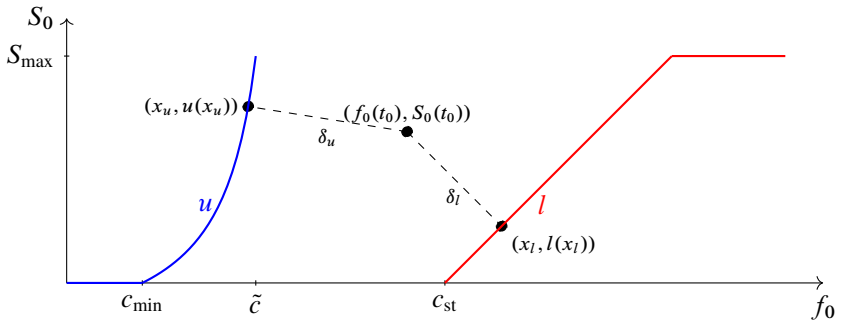

Figure 4. An f_0–S_0 phase diagram: example for $(f_0(t_0), S_0(t_0))$ and x_u and x_l.

and that the weak convergence of v_{ε_k} is actually strong. As a consequence, v_0 solves the limiting evolution equation

$$\begin{aligned} \partial_t v_0 - D\Delta v_0 &= \Lambda\Big(\frac{c(S_0, N_0, F)}{c_{\min}} - 1\Big)v_0 && \text{in } (0,T)\times\Omega, \\ \partial_\nu v_0 &= 0 && \text{on } (0,T)\times\partial\Omega, \\ v_0(0) &= v_{\mathrm{in}} && \text{on } \Omega. \end{aligned}$$

We now analyse the limiting behaviour of S_0 as a function of $f_0 = F/N_0$. Assume first that at a time $t_0 \in [0,T]$, the point $(f_0(t_0), S_0(t_0))$ is located in the f_0–S_0 phase-space diagram between the graphs $(x, l(x))$ for $x \geq c_{\mathrm{st}}$ and $(x, u(x))$ with $x \leq \tilde{c}$; cf. Figure 4 and recall that $S_0 \leq S_{\max}$.

We will show that this assumption implies $\dot{S}_0 = 0$ a.e. on a sufficiently small interval J with $t_0 \in J$: for the point $(f_0(t_0), S_0(t_0))$, we introduce any nearest point $(x_u, u(x_u))$ and the associated distance δ_u, i.e.

$$\delta_u = \|(x_u, u(x_u)) - (f_0(t_0), S_0(t_0))\| \quad \text{with } x_u \in \operatorname*{argmin}_{x, x\leq\tilde{c}} \|(x, u(x)) - (f_0(t_0), S_0(t_0))\|.$$

Note that $(x_u, u(x_u))$ is unique due to the convexity of u. However, the following argument also holds for general increasing functions u. Analogously, we define any nearest point $(x_l, l(x_l))$ and its distance δ_l. Again, $(x_l, l(x_l))$ is unique due to the concavity of l, but the argument holds for general increasing functions l.

Due to the uniform convergence of f_{ε_k} to f_0 and of p_{ε_k} to S_0, as shown in Step 3, we can choose ε_0 sufficiently small such that for all $\varepsilon_k < \varepsilon_0$ there holds

$$|(f_{\varepsilon_k}, p_{\varepsilon_k}) - (f_0, S_0)| < \frac{1}{4}\min\{\delta_u, \delta_l\}$$

uniformly in $t \in [0,T]$. Hence, for all $\varepsilon_k < \varepsilon_0$, the point $(f_{\varepsilon_k}(t_0), p_{\varepsilon_k}(t_0))$ has a distance larger than $\frac{3}{4}\min\{\delta_u, \delta_l\}$ to the graphs $(x, l(x))$ for $x \geq c_{\mathrm{st}}$ and $(x, u(x))$ with $x \leq \tilde{c}$.

As a consequence, there exists an open interval $I \ni t_0$ such that for all $t \in I$ the distance between $(f_{\varepsilon_k}(t), p_{\varepsilon_k}(t))$ and the graphs $(x, l(x))$ and $(x, u(x))$ is greater than $\frac{1}{2}\min\{\delta_u, \delta_l\}$. From Steps 2 and 3, we know that $(f_{\varepsilon_k}(t), S_{\varepsilon_k}(t)) - (f_{\varepsilon_k}(t), p_{\varepsilon_k}(t))$ converges to zero a.e. in I. Moreover, f_{ε_k} converges uniformly to f_0 and is Lipschitz continuous with a modulus independent of ε_k. Therefore, there is some $t_1 \in I$, $t_1 < t_0$, with

$$|(f_{\varepsilon_k}(t_1), S_{\varepsilon_k}(t_1)) - (f_{\varepsilon_k}(t_1), p_{\varepsilon_k}(t_1))| < \frac{1}{4}\min\{\delta_u, \delta_l\}$$

for all ε_k sufficiently small (i.e. by eventually choosing ε_0 smaller). Moreover, for each ε_k and for some $t \in [0, T]$, if $(f_{\varepsilon_k}(t), S_{\varepsilon_k}(t))$ is located between the graphs $(x, l(x))$ and $(x, u(x))$, then S_{ε_k} remains constant until the first time $\tilde{t} > t$ when

$$S_{\varepsilon_k}(\tilde{t}) = u(f_{\varepsilon_k}(\tilde{t})) \quad \text{or} \quad S_{\varepsilon_k}(\tilde{t}) = l(f_{\varepsilon_k}(\tilde{t})).$$

With the Lipschitz modulus of f_{ε_k} being independent of ε_k, the trajectory $(f_{\varepsilon_k}, S_{\varepsilon_k})$ keeps, for all $\varepsilon_k < \varepsilon_0$, a positive distance to the graphs $(x, l(x))$ and $(x, u(x))$ on an interval $J := I \cap [t_1, T] \ni t_0$ if I is chosen sufficiently small. Furthermore, on J, it follows by definition that

$$S_{\varepsilon_k} = p_{\varepsilon_k} \text{ and } \dot{p}_{\varepsilon_k} = 0 \quad \text{a.e. in } J \text{ and for all } \varepsilon_k < \varepsilon_0.$$

Hence, for $t \in J$,

$$S_0(t) = \lim_{k\to\infty} p_{\varepsilon_k}(t) = \lim_{k\to\infty} p_{\varepsilon_k}(t_1) = S_0(t_1)$$

and $\dot{S}_0 = 0$ a.e. in J as claimed.

We will now consider the case when $S_0(t_0) = u(f_0(t_0))$: for $t \in [t_0 - \delta, t_0 + \delta]$ with δ chosen in (30) (which excludes (f_0, S_0) reaching the graph $(x, l(x))$ in $[t_0 - \delta, t_0 + \delta]$), we know from the uniform convergence of f_{ε_k} to f_0, that $\dot{S}_{\varepsilon_k}(t) \le 0$ for ε_k sufficiently small; cf. Figure 3. We claim that therefore

$$\dot{p}_{\varepsilon_k} \le 0 \quad \text{a.e. in } [t_0 - \delta, t_0 + \delta].$$

The proof assumes in contradiction that for some $t_1 < t_2 \in [t_0 - \delta, t_0 + \delta]$ and for some $0 < \varepsilon_k < \varepsilon_1$ for ε_1 chosen sufficiently small $p_{\varepsilon_k}(t_2) > p_{\varepsilon_k}(t_1)$. The ε_k-independent Lipschitz continuity of p_{ε_k} (see Step 1) implies the existence of a time $t_3 \in (t_1, t_2)$ and a constant $\delta_1 > 0$ such that

$$p_{\varepsilon_k}(t_2) - \delta_1 > p_{\varepsilon_k}(t) \quad \text{for all } t \in [t_1, t_3] \text{ and all } \varepsilon_k < \varepsilon_1,$$

with $0 < \varepsilon_1$ sufficiently small. Due to the a.e. pointwise convergence of S_{ε_k} to p_{ε_k}, there exists a time $t_4 \in [t_1, t_3]$ such that

$$S_{\varepsilon_k}(t_4) < p_{\varepsilon_k}(t_2) - \frac{\delta_1}{2} \quad \text{for all } \varepsilon_k < \varepsilon_1,$$

where ε_1 might again be chosen smaller. Now, because $\dot{S}_{\varepsilon_k} \leq 0$ on $[t_0 - \delta, t_0 + \delta]$, we have

$$S_{\varepsilon_k}(t) < p_{\varepsilon_k}(t_2) - \frac{\delta_1}{2} \quad \text{for all } t \in [t_4, t_2] \text{ and all } \varepsilon_k < \varepsilon_1.$$

In return, by using again that $S_{\varepsilon_k} - p_{\varepsilon_k}$ converges to zero a.e.,

$$p_{\varepsilon_k}(t) < p_{\varepsilon_k}(t_2) - \frac{\delta_1}{4} \quad \text{for a.e. } t \in [t_4, t_2] \text{ and all } \varepsilon_k < \varepsilon_1,$$

for ε_1 chosen sufficiently small. By the continuity of p_{ε_k}, this estimate holds for all $t \in [t_4, t_2]$, which gives the contradiction $p_{\varepsilon_k}(t_2) < p_{\varepsilon_k}(t_2) - \frac{\delta_1}{4}$. Hence, we have proven $\dot{p}_{\varepsilon_k} \leq 0$ a.e. in $[t_0 - \delta, t_0 + \delta]$ and for ε_k sufficiently small. Since p_{ε_k} converges to S_0 uniformly and star-weakly in $\mathrm{W}^{1,\infty}(0,T)$ due to Step 1, this also yields $\dot{S}_0 \leq 0$ a.e. in $[t_0 - \delta, t_0 + \delta]$.

Altogether, by combining the situations with $\dot{S}_0 = 0$ a.e. and $\dot{S}_0 \leq 0$ a.e., we have proven that $\dot{S}_0 < 0$ in a set of positive measure is only possible if a.e. in this set $S_0 = u(f_0)$. In the analogous case when $S_0(t_0) = l(f_0(t_0))$, it follows similarly that $\dot{S}_0 \geq 0$ and that $\dot{S}_0 > 0$ in a set of positive measure is only possible if a.e. in this set $S_0 = l(f_0)$.

Summarising, we have shown that S_0 satisfies for a.e. $t \in [0,T]$,

$$\dot{S}_0(t)(S_0(t) - z) \leq 0 \quad \text{for all } \begin{cases} z \in [0, u(f_0(t))] & \text{if } f_0(t) \leq \tilde{c}, \\ z \in [l(f_0(t)), S_{\max}] & \text{if } f_0(t) \geq c_{\mathrm{st}}, \end{cases}$$

$$\dot{S}_0(t) = 0 \qquad \text{if } \tilde{c} < f_0(t) < c_{\mathrm{st}}.$$

Because $0 \leq S_0 \leq S_{\max}$, this shows that v_0 and S_0 solve (10)–(15).

Step 5: Uniqueness of solutions (v_0, S_0) to the limiting system (10)–(15). The limit S_0 is a generalised play for the Lipschitz continuous curves $U = \min\{S_{\max}, u(f_0)\}$ and $L = \max\{0, l(f_0)\}$ with input $f_0 = F/N_0$. By [28, Chapter III.2, Theorem 2.2] this generalised play is a Lipschitz continuous hysteresis operator from $\mathrm{C}([0,T]) \times \mathbb{R}$ to $\mathrm{C}([0,T])$. Since $N_0(t) > \delta(T) > 0$ uniformly in $[0,T]$, the input $f_0 = F/N_0$ also is Lipschitz continuous. The uniqueness of (v_0, S_0) then follows by using a Grönwall argument; see e.g. [28].

The regularity properties of v_0 follow essentially as in the proof of Theorem 1. Since $f_0 \in \mathrm{W}^{1,\infty}(0,T)$, also $S_0 \in \mathrm{W}^{1,\infty}(0,T)$ by [28, Chapter III.2, Theorem 2.3].

Step 6: Convergence of the whole sequence $\varepsilon \to 0$. Because every sequence $\{\varepsilon\}$ with $\varepsilon \to 0$ has a subsequence $\{\varepsilon_k\}_k$ such that $v_{\varepsilon_k} \to v_0$ in $\mathrm{W}^{1,q}(0,T;\mathrm{L}^2(\Omega)) \cap \mathrm{L}^q(0,T;\mathrm{H}^2(\Omega))$ and $S_{\varepsilon_k} \to S_0$ in $\mathrm{L}^q(0,T)$, uniqueness of the limit implies convergence of the whole sequence $(v_\varepsilon, S_\varepsilon)$. ∎

4. Numerical examples and discussion

In this section we present selected examples of the behaviour of hysteresis–reaction–diffusion systems on the one-dimensional domain $\Omega = (0,1)$.

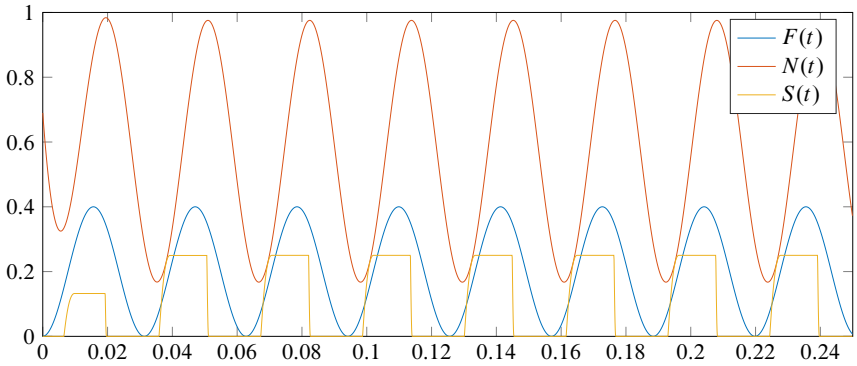

Figure 5. Evolution of the population–hysteresis–diffusion system (10)–(15): time-periodic food supply $F(t) = 0.2(1 - \cos(t))$ (blue) and the resulting population size N (red) and stock S (yellow).

Numerical method

All numerical examples are implemented and simulated in Matlab using a uniform mesh with 99 elements for the domain $\Omega = (0, 1)$. The discretised Neumann realisation of the Laplace operator $-\Delta$ is computed by a standard three-point stencil finite difference scheme and the corresponding discretised eigenfunctions ϕ_k, $k \geq 0$, together with their eigenvalues λ_k, can be computed by explicit formulas. The eigenfunctions are only used for the specification of initial data.

The hysteresis operator is approximated by an ODE regularisation of the variational inequality (34), similarly to [4] or [18]. As regularisation parameter we use $\varepsilon = 10^{-4}$. The resulting approximative ODE–reaction–diffusion equation is solved by a semi-implicit time-stepping procedure with implicit diffusion and explicit reaction with a step size $dt = 7.5 \times 10^{-5}$.

4.1. Simulation of the hysteresis–reaction–diffusion system (10)–(15)

The first example illustrates the population dynamical model (10)–(15) in the case of consumption rate function c_2 with parameters $c_{\min} = 0.35$, $c_{\mathrm{de}}^{\infty} = 0.4$, $c_{\mathrm{st}} = 0.45$ and $S_{\max} = 0.3$. In particular, the food supply is time periodic, given as $F(t) = 0.2(1 - \cos(t))$. Moreover, the initial data were set to $N_{\mathrm{in}} = 7$, $v_{\mathrm{in}} = N_{\mathrm{in}}\phi_1 + 2.5\phi_2 + 2.5\phi_3$ and $S_{\mathrm{in}} = 0$.

Figure 5 depicts the evolution of the scalar quantities F, N and S. More details can be observed in a simulation video (see supplementary material). The video shows the time evolution of v, S, F and $F/N(v)$. The upper plot in the video depicts the current location of $(F/N(v), S)$ (red dot) in phase space in relation to the upper (magenta) and lower (cyan) boundary curves of the limiting generalised play operator and it can be verified that S indeed approximates this generalised play operator. The legend also shows the current value of S (see also Figure 5), as well as the maximal value of S during the previous

cycle. The value is updated every time when S starts to decrease. The lower plot shows the evolution of the population density v (blue).

Discussion. We observe that the hysteresis cycles initially gain amplitude before saturating. Qualitatively speaking, the system seems to behave like a nonlinear oscillator, which adapts to the periodic external forcing within a transition phase.

The simulation video shows in more detail the interplay between the amplitude of the hysteresis cycles, the current stock level S (red), the individual food supply $f = F/N(v)$ (green) and the total food supply F (yellow). The legend also shows the current value of $|v - N(v)|_1 = \int_\Omega |v - N(v)|\,dx$, as well as its maximal value during the last cycle. Note that since $\int_\Omega (v - N(v)) = 0$, we can interpret $|v - N(v)|_1$ as a measure of the spatial inhomogeneity of the population density v. The video updates the maximal values of S, resp. $|v - N(v)|_1$ whenever they start to decrease.

We observe that although diffusion is clearly dominant since the maximal value of $|v - N(v)|_1$ decreases, the nonlinear coupling hysteresis–reaction leads nevertheless to large oscillations of $|v - N(v)|_1$. In fact, the following example will show that these nonlinear effects can be so strong as to prevent spatial homogenisation and lead to the growth of spatial inhomogeneities.

4.2. Interplay between scalar hysteresis and a reaction–diffusion equation

The subsequent examples detail the interplay between the geometric properties of the two defining boundary curves $\mathcal{U}$ and $\mathcal{L}$ (see below) of a generalised play operator and a reaction–diffusion model. For the sake of a clear discussion, our examples consider a simple hysteresis–reaction–diffusion model and compare the numerical simulation with a Fourier analysis of the analytic solution. Generalisations of our observations to systems of hysteresis–reaction–diffusion equations are possible.

4.2.1. A simple hysteresis–reaction–diffusion model. For $\Omega = (0, 1)$ and $D > 0$, we consider the hysteresis–reaction–diffusion equation

$$\begin{aligned} &\partial_t y - D\Delta y = Ry && \text{on } \Omega \times (0,\infty),\\ &\partial_\nu y = 0 && \text{on } \partial\Omega \times (0,\infty),\\ &y(0) = y_0 && \text{on } \Omega, \end{aligned} \tag{33}$$

where R is a generalised scalar play operator defined according to Lipschitz continuous and strictly monotone increasing boundary curve functions $\mathcal{U} > \mathcal{L}\colon \mathbb{R} \to \mathbb{R}$ (see e.g. [28, Chapter III.2]), i.e.

$$\begin{aligned} &R(0) = \min\bigl\{\max\{\mathcal{L}(\mathrm{T}y(0)), R_0\}, \mathcal{U}(\mathrm{T}y(0))\bigr\}, && R_0 \in \mathbb{R},\\ &\dot{R}(t)(R(t) - z) \le 0 \quad \text{for all} \quad z \in [\mathcal{L}(\mathrm{T}y(t)), \mathcal{U}(\mathrm{T}y(t))] && \text{for a.e. } t > 0,\\ &R(t) \in \bigl[\mathcal{L}(\mathrm{T}y(t)), \mathcal{U}(\mathrm{T}y(t))\bigr] && \text{for } t \ge 0. \end{aligned} \tag{34}$$

In (34), T is a linear and continuous functional on $\mathrm{L}^2(\Omega)$ which is independent of time. In particular, if defined on $C([0,\infty); \mathrm{L}^2(\Omega))$, we find that $(\mathrm{T}y)(t) = (\mathrm{T}y(\cdot, t))$ for $t > 0$

and $y \in C([0,\infty);\mathrm{L}^2(\Omega))$ serves as input to a scalar hysteresis operator. Accordingly, a more precise notation is $R = R(\mathrm{T}y, R_0)$ or $R(\mathrm{T}y)$ for short.

Specifically, we consider T to be a linear combination of Fourier coefficients of y in terms of the eigenfunctions $\{\phi_k\}_{k\geq 0}$ of the Neumann realisation of the Laplacian $-\Delta$ (see e.g. [1] and recall that the eigenfunctions $\{\phi_k\}_{k\geq 0}$ form an orthonormal basis of $\mathrm{L}^2(\Omega)$ while the eigenvalues satisfy $\lambda_0 = 0 < \lambda_1 < \lambda_2 < \cdots$ and $\lambda_k \to \infty$ as $k \to \infty$). Recalling that ϕ_0 is a positive constant and in view of the goal of studying the interplay between hysteresis and reaction, resp. diffusion, we consider T as a linear combination of Fourier coefficients $\langle u, \phi_k\rangle = \langle u, \phi_k\rangle_{\mathrm{L}^2((0,1))}$ of spatially inhomogeneous eigenfunctions $\{\phi_k(x)\}_{k\geq 1}$:

$$\mathrm{T}y := \underbrace{l_m}_{>0}\langle y, \phi_m\rangle + \sum_{i=m+1}^{M-1} \underbrace{l_i}_{\geq 0}\langle y, \phi_i\rangle + \underbrace{l_M}_{>0}\langle y, \phi_M\rangle, \quad 1 \leq m < M, \ \ m, M \in \mathbb{N}. \tag{35}$$

Another generic example for T could be the mean value functional $\mathrm{T}y = |\Omega|^{-1}\int_\Omega y(x)\,dx$.

The system (33)–(35) will be considered subject to nontrivial initial data $0 \neq y_0 \in \{v \in \mathrm{H}^2(\Omega) : \partial_\nu v = 0 \text{ on } \partial\Omega\}$. We choose y_0 to be a linear combination of eigenfunctions ϕ_k. In particular, we assume

$$\begin{aligned} &0 < y_0^{(m)} = \langle y_0, \phi_m\rangle, \quad 0 < y_0^{(M)} = \langle y_0, \phi_M\rangle \quad \text{and} \\ &0 \leq y_0^{(k)} = \langle y_0, \phi_k\rangle \quad \text{for } m < k < M, \text{ while } 0 = y_0^{(k)} \text{ for } 0 \leq k < m. \end{aligned} \tag{36}$$

Remark 10. The assumption $y_0^{(k)} = 0$ for $0 \leq k < m$ is made because those eigenmodes would have no effect on $R(\mathrm{T}y)$. However, those low eigenmodes have a strong influence on the large-time behaviour of y and would significantly complicate the interpretation of the results.

4.2.2. Spatial homogenisation versus spatially inhomogeneous large-time behaviour. In this section we show that geometric properties of generalised play operators (34) such as convexity/concavity or the slope of $\mathcal{U}$, resp. $\mathcal{L}$ can have a decisive influence on the evolution of the model (33)–(36). In particular, the scalar hysteresis operator (34) can decide between spatial homogenisation or unbounded growth of spatially inhomogeneous Fourier modes. This dichotomy is illustrated in Figures 6 and 7.

Description. Figures 6 and 7 depict a numerical simulation of system (33)–(36) subject to initial data $y_0 = (\phi_1 + \phi_2)/\|\phi_1 + \phi_2\|_{C([0,1])}$ and $R_0 = 0$. Moreover, we have set the diffusion coefficient and the parameters of the functional T in (35) to $D = \frac{1}{\lambda_1}$ and $m = 1$, $M = 2$, and $l_1 = 0.1$, $l_2 = 0.4$.

As boundary curves of the generalised play operator (34), we consider either a concave or a convex upper curve $\mathcal{U}$ and a concave lower curve $\mathcal{L}$:

$$\mathcal{U}_{\mathrm{cave}}(z) = 1.2|z|^{0.5}\mathrm{sign}(z) + 0.1, \quad \text{resp. } \mathcal{U}_{\mathrm{vex}}(z) = 0.1097|z|^2\mathrm{sign}(z) + 1.1468,$$
$$\mathcal{L}(z) = 1.2|z|^{0.5}\mathrm{sign}(z) - 0.1.$$

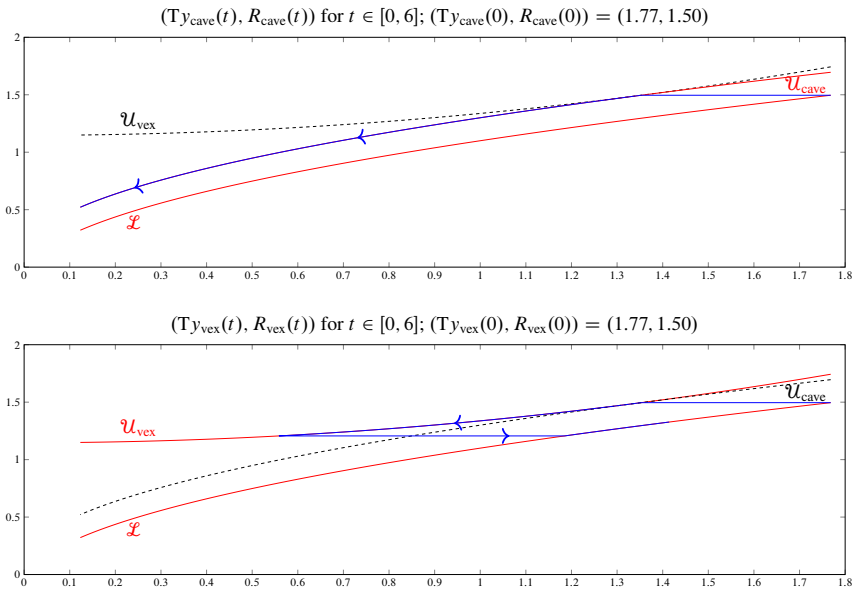

Figure 6. (*Top*) Phase-space evolution of $(\mathrm{T}y_{\mathrm{cave}}, R_{\mathrm{cave}})$ (blue) subject to $\mathcal{U}_{\mathrm{cave}}$ (upper red; black dashed $\mathcal{U}_{\mathrm{vex}}$ for comparison) and $\mathcal{L}$ (lower red). (*Bottom*) Phase-space evolution of $(\mathrm{T}y_{\mathrm{vex}}, R_{\mathrm{vex}})$ (blue) subject to $\mathcal{U}_{\mathrm{vex}}$ (upper red; black dashed $\mathcal{U}_{\mathrm{cave}}$ for comparison) and $\mathcal{L}$ (lower red). Both solutions start at the upper right end of the blue graphs at $(1.77, 1.5)$ and continue identically until hitting $\mathcal{U}_{\mathrm{cave}}$, resp. $\mathcal{U}_{\mathrm{vex}}$ at a point of identical slope. While the decay of $(\mathrm{T}y_{\mathrm{cave}}, R_{\mathrm{cave}})$ to zero yields spatial homogenisation, the turning of $(\mathrm{T}y_{\mathrm{vex}}, R_{\mathrm{vex}})$ leads to unbounded growth.

Note that the lack of Lipschitz continuity of $\mathcal{U}_{\mathrm{cave}}$ and $\mathcal{L}$ at zero is irrelevant since $\mathrm{T}y$ remains positive during the entire simulation.

In the following, we denote by $(y_{\mathrm{vex}}, R_{\mathrm{vex}})$ the solution of (33) subject to $\mathcal{U}_{\mathrm{vex}}$ and we denote by $(y_{\mathrm{cave}}, R_{\mathrm{cave}})$ the solution for $\mathcal{U}_{\mathrm{cave}}$. Figure 6 compares the $\mathrm{T}y$–R phase-space diagrams of two numerical solutions $(\mathrm{T}y_{\mathrm{vex}}, R_{\mathrm{vex}})$ and $(\mathrm{T}y_{\mathrm{cave}}, R_{\mathrm{cave}})$ both starting at the initial point $(1.77, 1.5)$. Hence, both solution trajectories initially move identically to the left at constant R-level and hit the upper boundary at the same time $t_+ = 0.15$, at a point where $\mathcal{U}_{\mathrm{cave}}$ and $\mathcal{U}_{\mathrm{vex}}$ share the same slope. With $\mathrm{T}y$ continuing to decrease, both solutions slide along their respective upper boundaries. While the top image in Figure 6 depicts the evolution of $(\mathrm{T}y_{\mathrm{cave}}, R_{\mathrm{cave}})$ according to the concave shape of $\mathcal{U}_{\mathrm{cave}}$, the lower image shows $(\mathrm{T}y_{\mathrm{vex}}, R_{\mathrm{vex}})$ following $\mathcal{U}_{\mathrm{vex}}$.

The key difference shown by Figure 6 is that the solution $(\mathrm{T}y_{\mathrm{cave}}, R_{\mathrm{cave}})$ continues to slide along $\mathcal{U}_{\mathrm{cave}}$ and thus converges to zero (see discussion below), while $(\mathrm{T}y_{\mathrm{vex}}, R_{\mathrm{vex}})$ features a turning point at time $t_0 = 1.34$ when $\mathrm{T}y_{\mathrm{vex}}$ starts to increase. In fact, $(\mathrm{T}y_{\mathrm{vex}}, R_{\mathrm{vex}})$ remains increasing, first at constant R-level, later sliding along the lower curve $\mathcal{L}$ and will thus become unbounded (see discussion below).

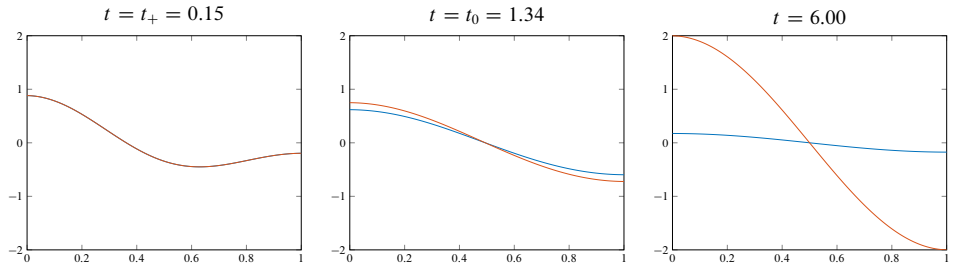

Figure 7. The solutions $y_{\text{cave}}(\cdot, t)$ (blue line) and $y_{\text{vex}}(\cdot, t)$ (brown line) of (33) subject to $\mathcal{U}_{\text{cave}}$, resp. $\mathcal{U}_{\text{vex}}$ at times $t = 0.15, 1.34, 6$. Being identical until $t_+ = 0.15$, y_{cave} converges to zero, while y_{vex} starts to grow at $t_0 = 1.34$ and continues to grow afterwards.

Figure 7 shows a plot of the corresponding solution $y_{\text{cave}}(\cdot, t)$ and $y_{\text{vex}}(\cdot, t)$ at selected times $t = 0.15, 1.34, 6$. Until $t_+ = 0.15$, both solutions are equal. Afterwards, $y_{\text{cave}}(\cdot, t)$ converges to zero, while $y_{\text{vex}}(\cdot, t)$ starts to grow.

Discussion and Fourier analysis. In order to analyse how the geometry of the scalar generalised play operator (34) governs the behaviour of the (nonlinear) reaction–diffusion equation (33), we expand y as a Fourier series in terms of the orthonormal basis $\{\phi_k\}_{k\geq 0}$ of $\mathrm{L}^2(0, 1)$, i.e.

$$y(x,t) = \sum_{k=0}^{\infty} y^{(k)}(t)\phi_k(x), \quad \text{with } y^{(k)}(t) = \langle y(\cdot,t), \phi_k(\cdot)\rangle.$$

Inserting into (33) yields for all k,

$$\begin{aligned} &\dot{y}^{(k)}(t) = \mu_k(t) y^{(k)}(t), \quad \text{with } \mu_k(t) := R(t) - D\lambda_k \text{ for a.e. } t > 0, \\ &y^{(k)}(0) = \langle y_0, \phi_k\rangle. \end{aligned} \tag{37}$$

In the following we demonstrate that the difference between y_{cave} and y_{vex} stems from a change of monotonicity of Fourier coefficients $y^{(k)}$, which is a consequence of the different decay of $R(t)$ (and hence of a different sign of some $\mu_k(t)$), as the solutions slide along $\mathcal{U}_{\text{cave}}$, resp. $\mathcal{U}_{\text{vex}}$.

The initial data set the monotonicity of the Fourier coefficients $y^{(k)}$ according to (37): with

$$\mu_k(0) := \min\big\{\max\{\mathcal{L}(\mathrm{T}y_0), R_0\}, \mathcal{U}(\mathrm{T}y_0)\big\} - D\lambda_k,$$

we assume initial data R_0, y_0 and weights l_i, $i = m, \dots, M$, with m and M from the definition of the functional T in (35) such that (as in the example in Figures 6 and 7)

$$\frac{d}{dt}(\mathrm{T}y)(0) = \sum_{i=m}^{M} l_i \mu_i(0) y_0^{(i)} < 0 \quad \text{and there exists } m < I_0 \leq M, \tag{38}$$

where

$$\mu_k(0) > 0 \ \text{ for } 0 \le k < I_0, \quad \text{and} \quad \mu_k(0) < 0 \ \text{ for } I_0 \le k \le M.$$

Note that the μ_k are monotone decreasing in k in the same way as the eigenvalues λ_k are monotone increasing. Hence, we introduce the *monotonicity index*

$$I(0) := I_0, \quad I(t) := \begin{cases} \min\{k \in \mathbb{N} : \mu_k(t) \le 0\} & \text{if } \mu_0(t) \ge 0, \\ -\infty & \text{if } \mu_0(t) < 0, \end{cases} \tag{39}$$

which points to the lowest nonincreasing Fourier mode $y^{(k)}$ for $k = 0, \dots, \infty$.

Remark 11. Note that $m \ge 1$ in (35) (Figures 6 and 7 use $m = 1$) implies that T focuses on the Fourier modes orthogonal to the lowest Fourier mode $y^{(0)}(t) = \langle y(\cdot, t), \phi_0 \rangle$, where ϕ_0 is a positive constant. Hence, while the zero-order Fourier mode $y^{(0)}(t) \sim \int_\Omega y(x,t)\,dx$ represents the total population, the higher-order Fourier modes $y^{(k)}(t)$ for $k \ge m$ determine whether the solution y converges to a space-homogeneous large-time behaviour. The example of Figures 6 and 7 shows that despite being spatially homogeneous, the hysteresis operator (34) may not only prevent spatial homogenisation but yield growth of higher Fourier modes, i.e. Fourier modes become unbounded in infinite time. We emphasise that (33) is a scalar PDE and that the observed mechanism of conditional spatial homogenisation versus spatially inhomogeneous large-time behaviour is quite different to e.g. Turing instability.

In Figures 6 and 7, since $y_0^{(m)}, y_0^{(M)} > 0$ and (37), (38) are satisfied, the Fourier coefficient $y^{(m)}(t)$ is strictly increasing while $y^{(M)}(t)$ is strictly decreasing on some sufficiently small time interval. It also holds that

$$\frac{d}{dt}(\mathrm{T}y)(t) = \sum_{i=m}^{M} l_i \mu_i(t) y^{(i)}(t) < 0 \quad \text{for } t > 0 \text{ sufficiently small.} \tag{40}$$

The evolution (40) is determined by the values/signs of the involved Fourier coefficients $\mu_k(t) = R(t) - D\lambda_k$ and, hence, by the monotonicity index $I(t)$ defined in (39).

In return, the evolution of the $\mu_k(t)$ is governed by the evolution of $R(t)$ given by (34), i.e. $R(t)$ is constant if $R \in (\mathcal{L}(\mathrm{T}y(t)), \mathcal{U}(\mathrm{T}y(t)))$, strictly increasing if $R(t) = \mathcal{L}(\mathrm{T}y(t))$ and $\frac{d}{dt}(\mathrm{T}y)(t) > 0$, and strictly decreasing if $R(t) = \mathcal{U}(\mathrm{T}y(t))$ and $\frac{d}{dt}(\mathrm{T}y)(t) < 0$.

Remark 12. Before analysing the dichotomy of Figures 6 and 7, we note first that $\mathrm{T}y \in \mathrm{C}([0,T]) \cap \mathrm{C}^1(0,T)$ for any $T > 0$. Moreover, $R \in \mathrm{W}^{1,\infty}(0,T)$ and $\mathrm{T}y \in \mathrm{W}^{2,\infty}(0,T)$.

The following proposition provides a largely explicit analysis of the nonlinear behaviour depicted in Figures 6 and 7.

Proposition 13 (Spatial homogenisation versus fixed pattern versus unbounded growth). Case I, spatial homogenisation: *Assume that the monotonicity index $I(t)$ (39) drops to the value m at some positive time $t_m > 0$.*

Then $\frac{d}{dt}(\mathrm{T}y)$ *is negative for all* $t > t_m$. *As a consequence,* $R(t)$ *remains nonincreasing for all* $t > t_m$. *Moreover,* $y(x,t)$ *either converges to zero (at least) exponentially fast or in the special case that* $\mu_m(t_m) = 0$ *and that*

$$\mathrm{T}y(t_m) - \sum_{m+1}^{M} l_i y^{(i)}(t_m) e^{\mu_i(t_m)t_m} \geq \mathcal{U}^{-1}(R(t_m)) \tag{41}$$

holds, and then the overall decay in the input $\mathrm{T}y$ *of the hysteresis operator* R *is too small to reach the upper boundary* $\mathcal{U}$. *This implies* $R(t) = R(t_0)$ *for all* $t > t_m$ *and the population density* $y(x,t)$ *converges to* $y^{(m)}(t_m)\phi_m(x)$.

Case II, growth: *Case I does not occur and the monotonicity index* $I(t)$ *remains larger than* m.

Then the ordering of the $\mu_k(t)$ *implies in* (40) *that* $\mathrm{T}y$ *stops decreasing at some time* $t_0 > 0$, *i.e.* $\frac{d}{dt}(\mathrm{T}y)(t_0) = 0$. *Consequently, for* $t > t_0$, $\mathrm{T}y(t)$ *increases and* $R(t)$ *is constant at first and increasing later, once* $R(t) = \mathcal{L}(\mathrm{T}y(t))$. *The growth of* $\mathrm{T}y$ *does not stop and so continues the consequential growth of* $R(t) = \mathcal{L}(\mathrm{T}y(t))$. *Hence, all* $\mu_k(t)$, $k \geq m$ *become positive after finite time and the corresponding Fourier modes* $y^{(k)}(t)$ *grow exponentially fast. The leading-order contribution, however, is always given by* $y^{(m)}(t)\phi_m(x)$.

Proof. Case I. If the monotonicity index $I(t_m) = m$ for some $t_m > 0$, then $\mu_m(t_m) \leq 0$ and $\mu_k(t_m) < 0$ for $m < k < \infty$. Hence, (40) yields $\frac{d}{dt}(\mathrm{T}y)(t_m) < 0$ (since $l_M > 0$) and $\mathrm{T}y \in \mathrm{C}^1(0,T)$ (recall Remark 12) implies $\frac{d}{dt}(\mathrm{T}y)(t) < 0$ on a sufficiently small interval $t \in [t_m, t_m + \varepsilon)$. Therefore, $\dot{R}(t) \leq 0$ a.e. on $[t_m, t_m + \varepsilon)$ since R can only increase if $R = \mathcal{L}(\mathrm{T}y)$ and $\frac{d}{dt}(\mathrm{T}y) > 0$. Consequently, $\mu_m(t) = R(t) - D\lambda_k \leq \mu_m(t_m) \leq 0$ on $[t_m, t_m + \varepsilon)$ and therefore $I(t) \leq m$ on $[t_m, t_m + \varepsilon)$. Note that if $\mu_m(t_m) < 0$, then $\mu_m(t) < 0$ for all $t > t_m$ since R is nonincreasing and all Fourier modes $y^{(k)}(t)$ for $m \leq k \leq M$ and thus $\mathrm{T}y(t) = \sum_{i=m}^{M} l_i y^{(i)}(t)$ decay (at least) exponentially fast to zero. Therefore $R(t)$ and $y(x,t)$ converge (at least) exponentially fast to zero.

On the other hand, if $\mu_m(t_m) = 0$, it depends on the accumulated decay of $\mathrm{T}y$ whether $R(t) = R(t_0)$ and thus $\mu_m(t) = \mu_m(t_m) = 0$ for all $t > t_m$ or whether there exists a time $t_- \geq t_m$ when $R(t_-) = \mathcal{U}(\mathrm{T}y(t_-))$, after which $R(t) < R(t_-)$ and $\mu_m(t) < \mu_m(t_-) = 0$ for $t > t_-$. In the second case – as above – it follows from then on that $\mathrm{T}y(t)$ and $R(t)$ and $y(x,t)$ converge (at least) exponentially to zero. In the first case, we note that $R(t)$ and all eigenvalues μ_k are constant in time as long as the hysteresis has not reached the upper boundary. Accordingly, we integrate (40) using (37):

$$\begin{aligned}\mathrm{T}y(t) &= \mathrm{T}y(t_m) + \int_{t_m}^{t} \sum_{m}^{M} l_i \mu_i(t_m) y^{(i)}(t_m) e^{\mu_i(t_m)s}\, ds \\ &= \mathrm{T}y(t_m) + \sum_{m+1}^{M} l_i y^{(i)}(t_m)(e^{\mu_i(t_m)t} - e^{\mu_i(t_m)t_m}).\end{aligned}$$

Hence, under condition (41), the hysteresis will remain bounded away from the upper boundary for all times $t > t_m$, which in return implies $R(t)$ is constant and $\mu_m(t) = 0$ for all time $t > t_m$ and $y(x,t)$ converges to $y^{(m)}(t_0)\phi_m(x)$.

Case II: If Case I does not apply then $I(t) > m$ holds and the exponential growth of the Fourier coefficient $y^{(m)}(t)$ versus the exponential decay of $y^{(k)}(t)$ for $k \geq I(t)$ implies the existence of a time $t_0 > 0$ such that $\frac{d}{dt}(\mathrm{T}y)(t_0) = 0$, as well as $\frac{d}{dt}(\mathrm{T}y)(t) > 0$ and $\dot{R}(t) \geq 0$ a.e. on some time interval $t \in (t_0, t_0 + \varepsilon)$. The latter implies that the $\mu_k(t)$ and thus the monotonicity index $I(t)$ are nondecreasing in time. Hence we can iterate this argument and obtain $\frac{d}{dt}(\mathrm{T}y)(t) > 0$ for all $t > t_0$ and $\dot{R}(t) \geq 0$ for a.e. $t > t_0$. In particular, $R(t)$ remains constant equal to $R(t) = R(t_0)$ for all $t \geq t_0$ until a time $t_- > t_0$ when $R(t_-) = \mathcal{L}(\mathrm{T}y(t_-))$. Afterwards, for $t \geq t_-$, $R(t)$ increases according to $R(t) = \mathcal{L}(\mathrm{T}y(t))$. It follows that $I(t) > M$ after some finite time and all Fourier modes $y^{(k)}(t)$, $m \leq k \leq M$ grow exponentially. However, the main contribution to the solution y is again given by $y^{(m)}(t)\phi_m(x)$. ∎

Qualitative analysis of Figures 6 and 7. In the view of Proposition 13, Figure 6 can now be interpreted more explicitly: after the identical initial decay of $(\mathrm{T}y_{\mathrm{vex}}, R_{\mathrm{vex}})$ and $(\mathrm{T}y_{\mathrm{cave}}, R_{\mathrm{cave}})$ until hitting the upper boundary $\mathcal{U}$ at $t_+ = 0.15$, it is the different decay of $R_{\mathrm{cave}} = \mathcal{U}_{\mathrm{cave}}(\mathrm{T}y_{\mathrm{cave}})$ and $R_{\mathrm{vex}} = \mathcal{U}_{\mathrm{vex}}(\mathrm{T}y_{\mathrm{vex}})$, which yields that $R_{\mathrm{cave}}(t_m) = D\lambda_1 = 1$ at some time $t_m > t_+$ at which the monotonicity index satisfies $I(t_m) = m$ and Case I in Proposition 13 applies to $(\mathrm{T}y_{\mathrm{cave}}, R_{\mathrm{cave}})$.

On the other hand, $\mathrm{T}y_{\mathrm{vex}}$ has a turning point at $t_0 = 1.34$ and starts to increase again after t_0 with $R_{\mathrm{vex}}(t) = \mathcal{U}_{\mathrm{vex}}(\mathrm{T}y_{\mathrm{vex}}(t_0))$ constant. Note that the plot shows $R_{\mathrm{vex}}(t) > 1$ and thus $I(t) > m$ for all $t \geq 0$. Therefore, $\mathrm{T}y_{\mathrm{vex}}$ grows monotonically as discussed in Case II in Proposition 13. At time $t_- = 5.31$, $(\mathrm{T}y_{\mathrm{vex}}, R_{\mathrm{vex}})$ hits the graph of $\mathcal{L}$, and $\mathrm{T}y_{\mathrm{vex}}$ increases further for $t \geq t_-$ with $R_{\mathrm{vex}}(t) = \mathcal{L}(\mathrm{T}y_{\mathrm{vex}}(t))$.

4.3. Generalisations

Under an additional assumption on $\mathcal{U}$, $\mathcal{L}$, Proposition 13 extends to cases with initially increasing $\mathrm{T}y$.

Corollary 14 (Example with initially increasing $\mathrm{T}y$). *Assume the upper boundary curve $\mathcal{U}$ of the generalised play operator (34) is a strictly monotone increasing function with $\mathcal{U}(0) > 0$, which is point symmetric at $(0, \mathcal{U}(0))$, and set $\mathcal{L} = \mathcal{U} - 2\mathcal{U}(0)$. Then the following point symmetry holds: replace $l_m, l_M > 0$ and $l_{m+1}, \ldots, l_{M-1} \geq 0$ in (35) by $l_m, l_M < 0$ and $l_{m+1}, \ldots, l_{M-1} \leq 0$ to obtain an operator $\widetilde{\mathrm{T}}$. With $R = R(\mathrm{T}y)$ where y solves (33), we obtain $R(\mathrm{T}y) = -R(\widetilde{\mathrm{T}}y) =: -\widetilde{R}$. Consider the modified evolution problem*

$$\partial_t y - D\Delta y = -\widetilde{R}y, \quad \partial_\nu y = 0, \; y(0) = y_0. \tag{42}$$

Then the new solution $\tilde{y}$ of (42) equals the solution y of (33) with $l_m, l_M > 0$ and with $l_{m+1}, \ldots, l_{M-1} \geq 0$. But now, $\widetilde{\mathrm{T}}\tilde{y} < 0$ is initially increasing. Moreover, in the phase-

space diagram of $\widetilde{\mathrm{T}}\tilde{y}$ *and* $\widetilde{R}$*, the new solution* $(\widetilde{\mathrm{T}}\tilde{y}, \widetilde{R})$ *is obtained by reflecting the old solution* $(\mathrm{T}y, R)$ *at the origin. In Case I,* $\widetilde{\mathrm{T}}\tilde{y} < 0$ *is always increasing so that* $\tilde{y}$ *converges to zero. In Case II,* $\widetilde{\mathrm{T}}\tilde{y}$ *is increasing until* t_0*, and then decreasing, which leads to growth of* $-\tilde{y} = |\tilde{y}|$.

4.3.1. General influence of slope and curvature. The example in Section 4.2.2 is constructed in such a way that the difference in the curvature of $\mathcal{U}$ is responsible for spatial homogenisation versus unbounded growth of solutions to (33)–(36). However, analogous examples can be constructed with different slopes of $\mathcal{U}$ deciding the large-time behaviour of solutions. The corresponding evolution of y depends mainly on the following two properties of $\mathcal{U}$:

- Is $\mathcal{U}(z)$ convex, linear or concave near $z = \mathrm{T}y(t_+)$?
- What is the slope $\mathcal{U}'(z)$ at $z = \mathrm{T}y(t_+)$ (or near $z = \mathrm{T}y(t_+)$ if $\mathcal{U}'(\mathrm{T}y(t_+))$ is not defined)?

Discussion. Assume, analogously to Figures 6 and 7, that the evolution of various solutions y, $\mathrm{T}y$ and R is identical for $t \in [0, t_+]$ independently from the considered curve $\mathcal{U}$. After t_+, the solutions $(\mathrm{T}y, R)$ slide in the phase-space diagram along the graphs of those curves $\mathcal{U}$ at least for a short distance as long as $\mathrm{T}y$ decreases, no matter whether Case I or Case II applies:

Steep $\mathcal{U}$. If $\mathcal{U}(z)$ is "steep" near $z = \mathrm{T}y(t_+)$, then $R(t)$ decreases "fast" compared to $\mathrm{T}y(t)$ for $t > t_+$. Hence, as long as $\frac{d}{dt}(\mathrm{T}y)(t) = \sum_{i=m}^{M} l_i \mu_i(t) y^{(i)}(t) < 0$ with $R(t) = \mathcal{U}(\mathrm{T}y(t))$, also $\mu_k(t)$, $m \le k \le M$ decreases "fast" compared to the evolution of Fourier coefficients $y^{(k)}(t)$. If this decay happens sufficiently fast for given initial data, we will find $I(t_m) = m$ for some $t_m > t_+$ and thus behaviour as in Case I of Proposition 13 and y will converge to zero.

Flat $\mathcal{U}$. On the other hand, if $\mathcal{U}(z)$ is "flat" near $z = \mathrm{T}y(t_+)$, $R(t)$ decreases "slowly" compared to $\mathrm{T}y$ for $t > t_+$. Hence, as long as $\frac{d}{dt}(\mathrm{T}y)(t) < 0$ for $t > t_+$ also $\mu_k(t)$, $m \le k \le M$ decreases "slowly" compared to the evolution of $y^{(k)}(t)$. If this decay happens sufficiently slowly for given initial data, it yields $\frac{d}{dt}(\mathrm{T}y)(t_0) = 0$ while $I(t_0) > m$ for some $t_0 > t_+$. Thus, we observe behaviour as in Case II of Proposition 13 and y will grow unboundedly.

The above observations carry over readily to $\mathcal{U}$ having different curvatures. Even if $\mathcal{U}_{\mathrm{vex}}$ and $\mathcal{U}_{\mathrm{cave}}$ have the same slope at $z = \mathrm{T}y(t_+)$, we observe that a *sufficiently strongly convex* $\mathcal{U}_{\mathrm{vex}}$ will yield $\frac{d}{dt}(\mathrm{T}y)(t_0) = 0$ while $I(t_0) > m$ for some $t_0 > t_+$ and thus Case II and unbounded growth. On the other hand, *sufficiently strongly concave* $\mathcal{U}_{\mathrm{cave}}$ will imply $I(t_m) = m$ for some $t_m > t_+$ and, therefore, y will converge to zero as in Case I.

All these examples can be altered to take place at the lower boundary curve $\mathcal{L}$. Consider the point symmetric setting from Corollary 14 and the evolution problem (42). Suppose convex, resp. concave curves $\mathcal{L}$. Choose initial data and $\mathcal{U}$ in such a way that the first contact $\widetilde{R}(t_-) = \mathcal{L}(\mathrm{T}\tilde{y}(t_-))$ is identical for all considered curves $\mathcal{L}$. Moreover,

assume the evolution of $\tilde{y}$, $\mathrm{T}\tilde{y}$ and $\widetilde{R}$ to be equal for $t \in [0, t_-]$ independently of $\mathcal{L}$. Then we find analogously to above,

- for *sufficiently steep* $\mathcal{L}$ and for $\frac{d}{dt}(\mathrm{T}\tilde{y}) > 0$ such that $\widetilde{R}$ increases sufficiently fast compared to $\tilde{y}^{(k)}(t)$, the solution $\tilde{y}$ converges to zero as in Case I;
- for *sufficiently flat* $\mathcal{L}$ and $\frac{d}{dt}(\mathrm{T}\tilde{y}) > 0$, $\widetilde{R}$ increases slowly compared to $\tilde{y}^{(k)}(t)$, yielding Case II and unbounded growth of $|\tilde{y}|$;
- if $\mathcal{L}_{\mathrm{vex}}$ is *sufficiently convex*, then $\tilde{y}$ converges to zero according to Case I;
- if $\mathcal{L}_{\mathrm{cave}}$ is *sufficiently concave*, then Case II and unbounded growth of $|\tilde{y}|$ take place.

5. Existence, uniqueness and regularity of the solution (S, v) to (1)–(8)

In this section we consider arbitrary $\varepsilon > 0$ fixed and prove existence and uniqueness of nonnegative, strong solutions (S, v) to system (1)–(8). For any open set X, we denote by $\mathrm{C}^1(\bar{X})$ the space of bounded and uniformly continuous functions on X, which have bounded and uniformly continuous derivatives.

Proof of Theorem 1. We consider the Neumann realisation in $\mathrm{L}^2(\Omega)$ of the Laplace operator with domain $\mathrm{dom}(-D\Delta) \doteq \{v \in \mathrm{H}^2(\Omega) : \partial_\nu v = 0 \text{ on } \partial\Omega\}$; see e.g. [1, Introduction].

(I) Local existence of nonnegative solutions via Banach's fixed point theorem. For any $\alpha \in (0, 1]$ and sufficiently large $\omega > 0$, we introduce the notation

$$A^\alpha := (-D\Delta + \omega)^\alpha \colon X^\alpha \subset \mathrm{L}^2(\Omega) \to \mathrm{L}^2(\Omega), \quad \text{where } X^\alpha := \mathrm{dom}(A^\alpha).$$

The embeddings $X^\alpha \hookrightarrow \mathrm{H}^{2\alpha}(\Omega)$ are continuous for $0 < \alpha \le 1$, so that $X^\alpha \hookrightarrow \mathrm{C}^{0,\beta}(\bar{\Omega})$ for $\alpha > \frac{3}{4}$ and for some $\beta \in (0, 1)$ if the dimension d of Ω is less than or equal to 3; see e.g. [1, Introduction] or [14,23]. Let $\alpha \in (3/4, 1]$ be arbitrary but fixed. Then, for $v_1, v_2 \in X^\alpha$ and

$$N_i := N(v_i) = \int_\Omega v_i(x)\,dx,$$

we estimate for some constant $c > 0$,

$$|N_1 - N_2| \le \int_\Omega |v_1(x) - v_2(x)|\,dx \le c|\Omega|\,\|v_1 - v_2\|_{X^\alpha}. \tag{43}$$

Let $S_{\mathrm{in}} \in \mathbb{R}^+$ and $v_{\mathrm{in}} \in \mathrm{dom}(-D\Delta)$ with $v_{\mathrm{in}} \ge 0$ and $N_{\mathrm{in}} > 0$ be given and consider the closed ball

$$B_\delta^\alpha := \overline{B_{\mathbb{R}\times X^\alpha}((S_{\mathrm{in}}, v_{\mathrm{in}}), \delta)}$$

for some small $\delta > 0$ to be chosen. Note that $v_{\mathrm{in}} \in X^\alpha$ for any $\alpha \in (0, 1]$. If δ is small enough, then (43) implies $N(V) > 0$ for all $(S, V) \in B_\delta^\alpha$. Moreover, since λ is bounded on bounded sets and because F and λ are (locally) Lipschitz continuous, there exists

a time $T > 0$ together with constants C_0, C_α, $L_F = L_F(S_{\mathrm{in}}, v_{\mathrm{in}}, T) > 0$ and $L_\lambda = L_\lambda(S_{\mathrm{in}}, v_{\mathrm{in}}, T) > 0$ such that for arbitrary $(S_1, v_1), (S_2, v_2) \in B_\delta^\alpha$ and for all $0 \le t_1, t_2 \le T$, we estimate

$$\begin{aligned}
&\|\lambda(S_1, N_1, F(t_1))v_1 - \lambda(S_2, N_2, F(t_2))v_2\|_{\mathrm{L}^2(\Omega)} \\
&\quad \le |\lambda(S_1, N_1, F(t_1))|\|v_1 - v_2\|_{\mathrm{L}^2(\Omega)} \\
&\qquad + |\lambda(S_1, N_1, F(t_1)) - \lambda(S_2, N_2, F(t_2))|\|v_2\|_{\mathrm{L}^2(\Omega)} \\
&\quad \le C_0 C_\alpha \|v_1 - v_2\|_{X^\alpha} + L_\lambda(|S_1 - S_2| + |N_1 - N_2| + L_F|t_1 - t_2|)C_\alpha\|v_2\|_{X^\alpha} \\
&\quad \le C_\alpha\Big(\frac{C_0}{c|\Omega|} + L_\lambda(2\delta + \|v_{\mathrm{in}}\|_{X^\alpha})\Big)(|S_1 - S_2| + c|\Omega|\|v_1 - v_2\|_{X^\alpha} + L_F|t_1 - t_2|) \\
&\quad \le C_1(|S_1 - S_2| + \|v_1 - v_2\|_{X^\alpha} + |t_1 - t_2|).
\end{aligned}$$

Note that the above estimate holds equally when replacing the left-hand-side norm $\mathrm{L}^2(\Omega)$ by X^α. We remark, moreover, that if λ were space dependent but sufficiently smooth, an estimate of the same form could be shown for $\mathrm{L}^2(\Omega)$ replaced by $\mathrm{dom}(-D\Delta)$ if $\alpha = 1$. Continuing the proof of Theorem 1 for spatially homogeneous λ, the above estimate proves that the mapping $(S, v, t) \to \lambda(S, N(v), F(t))v$ is Lipschitz continuous from $B_\delta^\alpha \times [0, T]$ into $\mathrm{L}^2(\Omega)$.

Similarly, we obtain

$$\begin{aligned}
&\big|F(t_1) - F(t_1)N_1 c(S_1, N_1, F(t_1)) - \big(F(t_2) - F(t_2)N_2 c(S_2, N_2, F(t_2))\big)\big| \\
&\quad \le |F(t_1) - F(t_2)|\,|1 + N_1 c(S_1, N_1, F(t_1))| \\
&\qquad + |F(t_2)|\,|N_1 c(S_1, N_1, F(t_1)) - N_2 c(S_2, N_2, F(t_2))| \\
&\quad \le L_F|t_1 - t_2|C_2 + F_{\max}|N_1 - N_2|\,|c(S_1, N_1, F(t_1))| \\
&\qquad + F_{\max}|N_2|\,|c(S_1, N_1, F(t_1)) - c(S_2, N_2, F(t_2))| \\
&\quad \le C_4(|S_1 - S_2| + \|v_1 - v_2\|_{X^\alpha} + |t_1 - t_2|),
\end{aligned}$$

where we used $|1 + N_1 c(S_1, N_1, F(t_1))| < C_2$ independently of $(S_1, v_1, t_1) \in B_\delta^\alpha \times [0, T]$, as well as (43). W.l.o.g. we can choose $C_4 = C_1$ from above.

In the following, we set $\alpha = 1$, denote $A := -D\Delta$, extend λ and c to arbitrary functions on $\mathbb{R} \times \mathbb{R} \times \mathbb{R}^+$ and reformulate system (1)–(8) in terms of $x = Av$ (see e.g. [23, Section 6.3]) and define the mild-formulation mapping

$$\begin{cases}
\Phi\colon \mathrm{C}([0, T]; \mathbb{R} \times \mathrm{L}^2(\Omega)) \to \mathrm{C}([0, T]; \mathbb{R} \times \mathrm{L}^2(\Omega)), \\
\Phi(S, x)(t) := \begin{pmatrix} S_{\mathrm{in}} + \dfrac{1}{\varepsilon}\displaystyle\int_0^t \big[F(\tau) - N(A^{-1}x(\tau))c\big(S(\tau), N(A^{-1}x(\tau)), F(\tau)\big)\big]\,d\tau \\ e^{t(-A)}Av_{\mathrm{in}} + \int_0^t e^{(t-\tau)(-A)}\lambda(S(\tau), N(A^{-1}x(\tau)), F(\tau))x(\tau)\,d\tau \end{pmatrix}.
\end{cases}$$

Next we introduce the closed set Σ,

$$\begin{aligned}
\Sigma := \big\{(S, x) \in \mathrm{C}([0, T]; \mathbb{R} \times \mathrm{L}^2(\Omega)) : (S(0), x(0)) = (S_{\mathrm{in}}, Av_{\mathrm{in}}),\ S \ge 0, \\
\|(S, x) - (S_{\mathrm{in}}, Av_{\mathrm{in}})\|_{\mathrm{C}([0,T];\mathbb{R}\times\mathrm{L}^2(\Omega))} \le \delta\big\}.
\end{aligned}$$

Then, for $T, \delta > 0$ small enough, the Lipschitz continuity of $N\colon \mathrm{dom}(-D\Delta) \to \mathbb{R}$ (see (43)) implies that $N(A^{-1}x) > 0$ at every time $t \in [0,T]$ and for all $x \in \Sigma$. Moreover, the Lipschitz continuity of $(S,v,t) \mapsto \lambda(S,N(v),F(t))v \in \mathrm{dom}(-D\Delta)$ and of $(S,v,t) \mapsto F(t) - c(S,N(v),F(t))N(v) \in \mathbb{R}$ in a neighbourhood of $(S_{\mathrm{in}}, v_{\mathrm{in}}, 0)$ in $\mathbb{R} \times \mathrm{dom}(-D\Delta) \times [0,T]$, yields (for sufficiently small T) that Φ maps the closed set Σ into itself and that Φ is a contraction.

Therefore, Banach's fixed point theorem yields a unique fixed point $(S,x) \in \Sigma$ of Φ. Note that since $S_{\mathrm{in}} \geq 0$, the quasi-positivity property (3), i.e. $(F - Nc(0,N,F))_- = 0$ and the local Lipschitz continuity of $(S,v,t) \to F(t) - N(v(t))c(S(t),N(v(t)),F(t))$ ensure that $S \geq 0$ holds on $[0,T]$ independently of T.

The function $t \mapsto \lambda(S(t),N(A^{-1}x(t)),F(t))A^{-1}x(t)$ is in $\mathrm{C}([0,T];\mathrm{L}^2(\Omega))$. With some additional work (see e.g. [23]) one can show that $t \mapsto x(t) \in \mathrm{L}^2(\Omega)$ is locally Hölder continuous for $t \in (0,T]$. Hence, S is locally Lipschitz continuous and so is the function $t \mapsto \lambda(S(t),N(A^{-1}x(t)),F(t))A^{-1}x(t) \in \mathrm{L}^2(\Omega)$ for $t \in (0,T]$. This implies that the linear inhomogeneous problem

$$\dot{w} + Aw = \lambda(S,N(A^{-1}x),F(\tau))A^{-1}x, \quad w(0) = v_{\mathrm{in}}$$

has a unique solution $w \in \mathrm{C}([0,T];\mathrm{L}^2(\Omega)) \cap \mathrm{C}^1((0,T];\mathrm{L}^2(\Omega))$, given by

$$w(t) = e^{t(-A)}v_{\mathrm{in}} + \int_0^t e^{(t-\tau)(-A)}\lambda(S,N(A^{-1}x),F(\tau))A^{-1}x\,d\tau.$$

Applying A to this equation shows that $w = A^{-1}x$, which implies that the function w solves (5)–(7). Moreover, $w \in \mathrm{C}([0,T];\mathrm{dom}(-D\Delta)) \cap \mathrm{C}^1((0,T];\mathrm{L}^2(\Omega))$. Since w is unique, this proves that

$$(S,v) := (S,w) \in \mathrm{C}\big([0,T];\mathbb{R} \times \mathrm{dom}(-D\Delta)\big) \cap \mathrm{C}^1\big((0,T];\mathbb{R} \times \mathrm{L}^2(\Omega)\big)$$

is the unique local solution of (1)–(8). Having already shown $S(t) \geq 0$, we are left to prove that the solution v of (5)–(7) satisfies $v(t,x) \geq 0$ for all $t \in [0,T]$ and all $x \in \overline{\Omega}$. Note first that $|\lambda(S(t),N(t),F(t))| \leq C$ uniformly in $t \in [0,T]$ for some $C > 0$. Let $\mu < -C$ be chosen arbitrarily and introduce the auxiliary function $\tilde{v} = ve^{\mu t}$. This function solves the evolution equation

$$\begin{cases} \partial_t \tilde{v}(t,x) - D\Delta\tilde{v}(t,x) = (\lambda(S,N,F) + \mu)\tilde{v}(t,x) \leq 0 & \text{a.e. in } (0,T) \times \Omega, \\ \partial_\nu \tilde{v}(t,x) = 0 & \text{a.e. in } (0,T) \times \partial\Omega, \end{cases} \tag{44}$$

subject to nonnegative initial data $\tilde{v}_{\mathrm{in}} \geq 0$. Moreover, $|\lambda(S(t),N(t),F(t))| + \mu \leq C + \mu < 0$ uniformly in $[0,T]$. Hence, by using weak parabolic maximum principle arguments (see e.g. [6]), we test (44) with $\tilde{v}_- = \min\{0,\tilde{v}\}$ and obtain after integration by parts,

$$\frac{d}{dt}\int_\Omega \frac{(\tilde{v}_-)^2}{2}\,dx \leq -D\int_\Omega |\nabla(\tilde{v}_-)|^2\,dx + (|\lambda| + \mu)\int_\Omega (\tilde{v}_-)^2\,dx \leq 0.$$

Hence $(\tilde{v}_{\mathrm{in}})_- = 0$ implies that $\tilde{v}_- = 0$ a.e. on Ω for all $t > 0$. Since $v \in \mathrm{C}([0,T] \times \overline{\Omega})$, this yields $v(t,x) \geq 0$ for all $t \in [0,T]$ and $x \in \overline{\Omega}$.

(II) Higher regularity and strong solutions. Since

$$(S, v, t) \mapsto \begin{pmatrix} \frac{1}{\varepsilon}(F(t) - N(v)c(S, N(v), F(t))) \\ \lambda(S, N(v), F(t))v \end{pmatrix}$$

is locally Lipschitz continuous into $\mathbb{R} \times \mathrm{L}^2(\Omega)$ on a neighbourhood of $(S_{\mathrm{in}}, v_{\mathrm{in}})$ in $\mathbb{R}^+ \times X^\alpha$ for any $0 < \alpha < 1$ and for $t > 0$, it follows by classical arguments that $t \mapsto \frac{d}{dt}v(t)$ is locally Hölder continuous into X^γ for any $0 < \gamma < 1$ and $t > 0$. As a consequence (see e.g. [14, Theorem 3.5.2]), it follows that

$$(S, v) \in \mathrm{C}\big([0, T]; \mathbb{R} \times \mathrm{H}^2(\Omega)\big) \cap \mathrm{C}^1\big((0, T]; \mathbb{R} \times \mathrm{C}^{0,\beta}(\bar{\Omega})\big), \tag{45}$$

where the exponent β is as defined in Theorem 1.

Note that the derivative $\dot{S}$ for $t > 0$ is given by

$$\dot{S}(t) = \frac{1}{\varepsilon}(F(t) - N(v(t))c(S(t), N(v(t)), F(t))),$$

and that the right-hand side is continuous and also bounded for $t \to 0$. Hence, $S \in \mathrm{C}^1([0, T])$.

(III) Global existence and lower bound for $N(v)$. The assumption that $c(S, N, F)$ is bounded along solutions implies that the nonlinear functions $t \mapsto \lambda(S(t), N(v(t)), F(t))v(t)$ and $t \mapsto F(t) - N(v(t))c(S(t), N(v(t)), F(t))$ satisfy at most linear growth estimates along solutions (S, v) of (1)–(8), which yields global existence of solutions by classical arguments; see e.g. [14, Corollary 3.3.5]. Moreover, estimate (9) shows for all $t \in [0, T]$ that $N(t) \geq N_{\mathrm{in}} \exp(-|\Lambda(-1)|T) =: \delta(T) > 0$.

(IV) Further regularity and classical solutions. For $t \in (0, T)$, we calculate

$$\begin{aligned} \frac{d}{dt}v(t) = -e^{t(-A)}Av_{\mathrm{in}} - \int_0^t e^{(t-\tau)(-A)}\lambda(S, N(v), F)Av\, d\tau \\ + \lambda(S(t), N(v(t)), F(t))v(t), \end{aligned} \tag{46}$$

and all functions on the right-hand side are contained in $\mathrm{C}([0, T]; \mathrm{L}^2(\Omega))$. Consequently, $\partial_t v$ is uniformly bounded in $\mathrm{L}^2(\Omega)$, i.e. $v \in \mathrm{C}^1([0, T]; \mathrm{L}^2(\Omega))$. Moreover, we recall that $t \mapsto \lambda(S(t), N(v(t)), F(t))$ is continuous and $\partial_t v(t), v(t) \in \mathrm{C}^{0,\beta}(\bar{\Omega})$ for all $t \in (0, T]$ from (II). Hence, for any fixed $t > 0$, we define $h(x) := -\partial_t v(t, x) + \lambda(S(t), N(t), F(t))v(t, x)$, and $v(t, .)$ solves the equation

$$\begin{cases} -D\Delta z(x) = h(x) & \text{for } x \in \Omega, \\ \partial_\nu z = 0 & \text{for } x \in \partial\Omega. \end{cases} \tag{47}$$

Moreover, $h \in \mathrm{C}^{0,\beta}(\bar{\Omega})$ satisfies the solvability condition $\int_\Omega h\, dx = 0$ since v solves (5)–(7). Thus, by [22, Theorem 3.1], problem (47) has a unique, normalised solution

$$z \in \mathcal{C} := \big\{v \in \mathrm{C}^{2,\beta}(\bar{\Omega}) : \textstyle\int_\Omega v(x)\, dx = N(u) = 0\big\}.$$

Moreover, [22, Theorem 4.1] yields that $\|z\|_{C^{2,\beta}(\bar{\Omega})} \le C\|h\|_{C^{0,\beta}(\bar{\Omega})}$ for a constant $C = C(\Omega, \beta, d) > 0$. Because $v(t,.)$ solves (47), the uniqueness of the normalised solution $z \in \mathcal{C}$ implies $z = v(t,.) - \frac{1}{|\Omega|}N(v(t))$. Therefore, the function $v(t,.)$ is contained in $C^{2,\beta}(\bar{\Omega})$ with

$$\begin{aligned}
&\Big\| v(t,.) - \frac{N(v(t,.))}{|\Omega|} \Big\|_{C^{2,\beta}(\bar{\Omega})} \\
&\quad \le C\|h\|_{C^{0,\beta}(\bar{\Omega})} \\
&\quad = C\| - \partial_t v(t,.) + \lambda(S(t), N(t), F(t))v(t,.)\|_{C^{0,\beta}(\bar{\Omega})} \\
&\quad \le C\| - \partial_t v(t,.)\|_{C^{0,\beta}(\bar{\Omega})} + C|\lambda(S(t), N(t), F(t))|\|v(t,.)\|_{C^{0,\beta}(\bar{\Omega})} < \infty.
\end{aligned}$$

Since the right-hand side is uniformly bounded for all $0 < t_0 \le t \le T$, we conclude $v \in L^\infty((t_0, T); C^{2,\beta}(\bar{\Omega}))$ for any $t_0 > 0$. Finally, $v \in C((0,T]; C^{2,\beta}(\bar{\Omega}))$ follows from a similar estimate and the observations that $t \mapsto \lambda(S(t), N(t), F(t))v(t) \in C([0,T]; C^{0,\beta}(\bar{\Omega}))$, $t \mapsto \frac{d}{dt}v(t) \in C((0,T]; C^{0,\beta}(\bar{\Omega}))$ and $t \mapsto N(v(t)) \in C([0,T])$. ∎

Funding. This work is supported by the International Research Training Group IGDK 1754 and NAWI Graz.

References

[1] H. Amann, *Linear and quasilinear parabolic problems. Vol. I*. Monogr. Math. 89, Birkhäuser, Boston, MA, 1995 Zbl 0819.35001 MR 1345385

[2] T. Aoki, Metabolic adaptations to starvation, semistarvation, and carbohydrate restriction. *Prog. Clin. Biol. Res.* **67** (1981), 161–77

[3] J. Betschinger, K. Mechtler, and J. Knoblich, The Par complex directs asymmetric cell division by phosphorylating the cytoskeletal protein Lgl. *Nature* **422** (2003), 326–329

[4] M. Brokate and P. Krejčí, Optimal control of ODE systems involving a rate independent variational inequality. *Discrete Contin. Dyn. Syst. Ser. B* **18** (2013), no. 2, 331–348 Zbl 1260.49002 MR 2999080

[5] M. Brokate and J. Sprekels, *Hysteresis and phase transitions*. Appl. Math. Sci. 121, Springer, New York, 1996 Zbl 0951.74002 MR 1411908

[6] M. Chipot, *Elements of nonlinear analysis*. Birkhäuser Adv. Texts Basler Lehrbücher, Birkhäuser, Basel, 2000 MR 1801735

[7] M. Curran, P. Gurevich, and S. Tikhomirov, Recent advance in reaction-diffusion equations with non-ideal relays. In *Control of self-organizing nonlinear systems*, pp. 211–234, Underst. Complex Syst., Springer, Cham, 2016 MR 3495765

[8] K. Disser, A. F. M. ter Elst, and J. Rehberg, Hölder estimates for parabolic operators on domains with rough boundary. *Ann. Sc. Norm. Super. Pisa Cl. Sci. (5)* **17** (2017), no. 1, 65–79 Zbl 1387.35324 MR 3676040

[9] P. Gurevich and D. Rachinskii, Asymptotics of sign-changing patterns in hysteretic systems with diffusive thresholds. *Asymptot. Anal.* **96** (2015), no. 1, 1–22 Zbl 1335.35121 MR 3437195

[10] P. Gurevich and D. Rachinskii, Pattern formation in parabolic equations containing hysteresis with diffusive thresholds. *J. Math. Anal. Appl.* **424** (2015), no. 2, 1103–1124 Zbl 1307.35039 MR 3292718

[11] P. Gurevich, R. Shamin, and S. Tikhomirov, Reaction-diffusion equations with spatially distributed hysteresis. *SIAM J. Math. Anal.* **45** (2013), no. 3, 1328–1355 Zbl 1276.35107 MR 3054588

[12] P. Gurevich and S. Tikhomirov, Systems of reaction-diffusion equations with spatially distributed hysteresis. *Math. Bohem.* **139** (2014), no. 2, 239–257 Zbl 1340.35136 MR 3238837

[13] P. Gurevich and S. Tikhomirov, Rattling in spatially discrete diffusion equations with hysteresis. *Multiscale Model. Simul.* **15** (2017), no. 3, 1176–1197 MR 3686776

[14] D. Henry, *Geometric theory of semilinear parabolic equations*. Lecture Notes in Math. 840, Springer, Berlin-New York, 1981 Zbl 0456.35001 MR 610244

[15] F. C. Hoppensteadt and W. Jäger, Pattern formation by bacteria. In *Biological growth and spread (Proc. Conf., Heidelberg, 1979)*, pp. 68–81, Lecture Notes in Biomath. 38, Springer, Berlin-New York, 1980 MR 609347

[16] F. C. Hoppensteadt, W. Jäger, and C. Pöppe, A hysteresis model for bacterial growth patterns. In *Modelling of patterns in space and time (Heidelberg, 1983)*, pp. 123–134, Lecture Notes in Biomath. 55, Springer, Berlin, 1984 MR 813709

[17] C. Kuehn, *Multiple time scale dynamics*. Appl. Math. Sci. 191, Springer, Cham, 2015 Zbl 1335.34001 MR 3309627

[18] C. Kuehn and C. Münch, Generalized play hysteresis operators in limits of fast-slow systems. *SIAM J. Appl. Dyn. Syst.* **16** (2017), no. 3, 1650–1685 Zbl 1381.34064 MR 3690648

[19] M. Mattson, V. Longo, and M. Harvie, Impact of intermittent fasting on health and disease processes. *Ageing Res. Rev.* **39** (2017), 46–58

[20] B. Mayer, G. Emery, D. Berdnik, F. Wirtz-Peitz, and J. Knoblich, Quantitative analysis of protein dynamics during asymmetric cell division. *Curr. Biology* **15** (2005), 1847–1854

[21] C. Münch, Global existence and Hadamard differentiability of hysteresis reaction-diffusion systems. *J. Evol. Equ.* **18** (2018), no. 2, 777–803 Zbl 06932122 MR 3820422

[22] G. Nardi, Schauder estimate for solutions of Poisson's equation with Neumann boundary condition. *Enseign. Math.* **60** (2014), no. 3-4, 421–435 Zbl 1317.35047 MR 3342652

[23] A. Pazy, *Semigroups of linear operators and applications to partial differential equations*. Appl. Math. Sci. 44, Springer, New York, 1983 Zbl 0516.47023 MR 710486

[24] A. Pimenov, T. C. Kelly, A. Korobeinikov, M. J. A. O'Callaghan, A. V. Pokrovskii, and D. Rachinskii, Memory effects in population dynamics: spread of infectious disease as a case study. *Math. Model. Nat. Phenom.* **7** (2012), no. 3, 204–226 Zbl 1316.92088 MR 2928740

[25] A. Rätz and B. Schweizer, Hysteresis models and gravity fingering in porous media. *ZAMM Z. Angew. Math. Mech.* **94** (2014), no. 7-8, 645–654 Zbl 1297.76168 MR 3230274

[26] D. Sartori, R. Migliorini, J. Veiga, J. Moura, I. Kettelhut, and C. Linder, Metabolic adaptations induced by long-term fasting in quails. *Comp. Biochem. Physiol. A Physiol.* **111** (1995), 487–493

[27] L. Tan, A. Acharya, and K. Dayal, Modeling of slow time-scale behavior of fast molecular dynamic systems. *J. Mech. Phys. Solids* **64** (2014), 24–43 MR 3159822

[28] A. Visintin, *Differential models of hysteresis*. Appl. Math. Sci. 111, Springer, Berlin, 1994 Zbl 0820.35004 MR 1329094

Received 10 April 2021; revised 23 December 2021; accepted 3 February 2022.

Klemens Fellner
Institute of Mathematics and Scientific Computing, University of Graz, Heinrichstraße 36, 8010 Graz, Austria; klemens.fellner@uni-graz.at

Christian Münch
Technical University of Munich, Boltzmannstraße 3, 85748 Garching bei München, Germany; chris_muench@gmx.de